A New Approach to the Computation of First Passage Time Distribution for Brownian Motion

by

Zhiyong Jin

A Thesis submitted to the Faculty of Graduate Studies of
The University of Manitoba
in partial fulfillment of the requirements of the degree of

MASTER OF SCIENCE

Department of Statistics
University of Manitoba
Winnipeg, Manitoba

Abstract

This thesis consists of two novel contributions to the computation of first passage time distribution for Brownian motion. First, we extend the known formula for boundary crossing probabilities for Brownian motion to the discontinuous piecewise linear boundary. Second, we derive explicit formula for the first passage time density of Brownian motion crossing piecewise linear boundary. Further, we demonstrate how to approximate the boundary crossing probabilities and density for general non-linear boundaries. Moreover, we use Monte Carlo simulation method and develop algorithms for the numerical computation. This method allows one to assess the accuracy of the numerical approximation. Our approach can be further extended to compute two-sided boundary crossing probabilities.

Acknowledgments

First and foremost I want to express my gratitude to my supervisor, Dr. Liqun Wang, for his extreme patience, inspirational advice and constant encouragement over the last several years, especially for his assistance in written scientific communications besides this thesis. Dr. Wang is also my life mentor, who has been motivating, enlightening and encouraging. He taught me how to deal with pressure and all the importance of organized working and thorough thinking.

I would like to thank committee members Dr. Brad Johnson and Dr. Alex Paseka for their kind support, generous assistance and helpful suggestions. I am grateful to Dr. Saumen Mandal and Dr. Xikui Wang for their encouragement in my graduate study.

Financial assistance from China Scholarship Council is also gratefully acknowledged.

Finally, but not least, I would like to give my sincere thanks to my parents and my sister for their love and encouragement throughout my life. In particular, I wish to express my heartfelt gratitude to my wife for her love and support.

Dedication

This thesis is dedicated to my beloved parents, sister, wife and son.

Contents

List of Tables

List of Figures

Chapter 1

Introduction

First passage time distributions for diffusion processes are also known as boundary crossing distributions, first hitting time or first exit time distributions. These distributions play an important role and have wide applications in many scientific disciplines ranging from environmental science, engineering, biology to finance. In environmental science, the first passage time is the main focus in many environmental processes such as the tidal communities life cycle, plant productivity, and outbreaks of waterborne diseases [3]. In engineering, first passage time distributions have applications in quality control and equipment failure analysis where the first passage time describes the life time until a quality measure first reaches a threshold [14]. In medicine and biology, the first passage time can be used to describe the length of stay in hospital [11] or the onset time of a cancer [8]. In mathematical finance, first passage time problems arise in barrier options pricing models [10, 13, 15, 18].

Depending on the real problems, sometimes the first passage time densities are concerned, while some other times the boundary crossing probabilities are desired.

However, the numerical computation of the first passage time distributions is challenging because explicit formulas exist in only a few special instances. Below, we introduce some concepts and notations that are central in this thesis.

1.1 Definitions and Notations of First Passage Time Distribution

Definition 1.1.1 (First Passage Time). *Let $X = \{X_s, s \geq 0, X_0 = x_0\}$ be a diffusion process defined on a probability space $(\Omega, \mathscr{A}, P)$ and X has either the real space $\mathbb{R}$ or a subinterval of $\mathbb{R}$ as its state space. Let $c(s), s \geq 0$ be a real function with $x_0 < c(0)$. The first passage time τ_c is defined as*

$$\tau_c = \min\{s \geq 0 : X_s \geq c(s)\}.$$

Definition 1.1.2 (Boundary Crossing Probability). *Let X, $c(s)$ and τ_c be defined as in Definition 1.1.1. For any fixed $t > 0$, the probability $P(\tau_c \leq t)$ is called the boundary crossing probability (BCP) on $[0, t]$. And it is given by*

$$\begin{aligned} P(\tau_c \leq t) &= P\left(X_s \geq c(s), \textit{ for some } s \in [0, t]\right) \\ &= 1 - P\left(X_s < c(s), \forall s \in [0, t]\right). \end{aligned}$$

For notational convenience, throughout this thesis we will denote the boundary non-crossing probability (BNCP) $P(\tau_c > t)$ for any $t > 0$ as

$$P_X(t; c) = P(X_s < c(s), \forall s \in [0, t]).$$

Therefore, the first passage time density (FPD) at $t \geq 0$, is the "rate of decrease" in time of $P_X(t;c)$.

Definition 1.1.3 (First Passage Time Density)**.** *Let X, $c(s)$, τ_c and $P_X(t;c)$ be defined as above, the first passage time density (FPD) at $t > 0$ is given by*

$$g_X(t;c) = -\frac{\partial P_X(t;c)}{\partial t}. \tag{1.1}$$

1.2 The Computational Challenge

Given the practical importance of the first passage time distributions, the numerical computation of these distributions is a difficult task. In the literature, many researchers have been trying to find either analytical or numerical solutions. Some other researchers develop simulation methods to find approximation solutions. However, the closed-form solutions for the first passage time distributions are unknown for general diffusion processes. An exception is Brownian motion and some special boundaries, for which the distribution of the first passage time can be obtained by a combination of Girsanov's theorem and the reflection principle ([16 2.6A]). Based on the Laplace transform for certain distributions [21], the image methods for the FPD have been used in [5, 7, 20, 27, 30]. These methods give exact results of both BNCP and FPD for Brownian motion and some special boundaries, e.g., the square-root boundary [27]. On the other hand, these methods strongly depend on the type of boundaries, because the accuracy of these methods depends on the accuracy of the approximation of the boundary. Moreover, for general diffusion processes the analytical forms of the Laplace transforms are quite difficult to obtain and sometimes even impossible.

Monte Carlo path simulation methods have been studied to compute the first passage time densities for general diffusion processes. The simplest scheme is called Euler scheme, in which first the process is discretized at predetermined grid time points $ih, i = 0, 1, \cdots$ where h is the step size, and then the sample paths are simulated and the number of crossing is counted. Further methods based on this were developed by Durbin [4] and Siegmund [28]. The problem with the simulation methods is that they require complicated algorithms and heavy computation and it is difficult to assess the approximation accuracies. Some other researchers consider the Monte Carlo simulation using Brownian bridge to approximate the BCP [23, 25] or FPD [12]. The Brownian bridge simulation method improves the efficiency of computation. But the analytical forms are not given and therefore the bound of the approximation can not be accessed, especially for the FPD.

In this thesis, we propose a new method to compute the BCP and FPD for Brownian motion, which can deal with general boundaries and is as fast as the Brownian bride simulation method. Firstly, we derive a new formula for the BCP for Brownian motion and piecewise linear boundaries that can be discontinuous. By combining this formula with the Fokker-Planck equation, we obtain a new explicit expression for the FPD of Brownian motion with discontinuous piecewise linear boundaries. Computation of these explicit formulas can be done using Monte Carlo simulation method, which is easy to implement and the accuracy of the approximation can be assessed and controlled. Moreover, for general boundaries we approximate the BNCP and FDP using approximating piecewise linear boundaries. Our methods can be further extended to compute two-sided boundary crossing probabilities, and can be applied to other diffusion processes such as Ornstein-Uhlenbeck processes, growth processes, geometric Brownian motion and even these processes combined with jump diffusions.

1.3 Thesis Organization

The structure of the thesis is as follows. In Chapter 2, we derive the explicit formulas of the BCP and FPD for Brownian motion and piecewise linear boundaries and propose a method to approximate the BNCP and FPD for general boundaries. In Chapter 3, we present Monte Carlo estimation algorithms and some examples with numerical results. Chapter 4 is concerned with the BNCP and FPD for diffusion processes which can be expressed as functionals of a standard Brownian motion. Chapter 5 is the summary. The MatLab programming codes are given in the Appendix.

Chapter 2

First Passage Time Distribution of Brownian Motion

In this chapter, we study the BNCP and FPD of the standard Brownian motion. We focus on three types of one-sided boundaries: linear boundary, piecewise linear boundary and general nonlinear boundary.

Wang and Poetzelberger [31] used a direct method to derive an explicit formula for the non-crossing probability for continuous piecewise linear boundaries. Using that formula they obtained approximation for general continuous boundaries. Following this method, we derive more general results of BNCP for piecewise linear boundaries which can be discontinuous. Based on these results, explicit formulas of FPD for piecewise linear boundaries are obtained. Further we use these results to approximate the BNCP and FPD for general (nonlinear) boundaries.

2.1 Introduction to Brownian Motion

In 1827, the Scottish botanist Robert Brown observed that a pollen particle suspended in liquid undergoes a strange erratic motion caused by bombardment by molecules of the liquid. Other scientists verified the strange phenomenon following Brown's initial report.

Figure 2.1: Example of sample paths of Brownian motion.

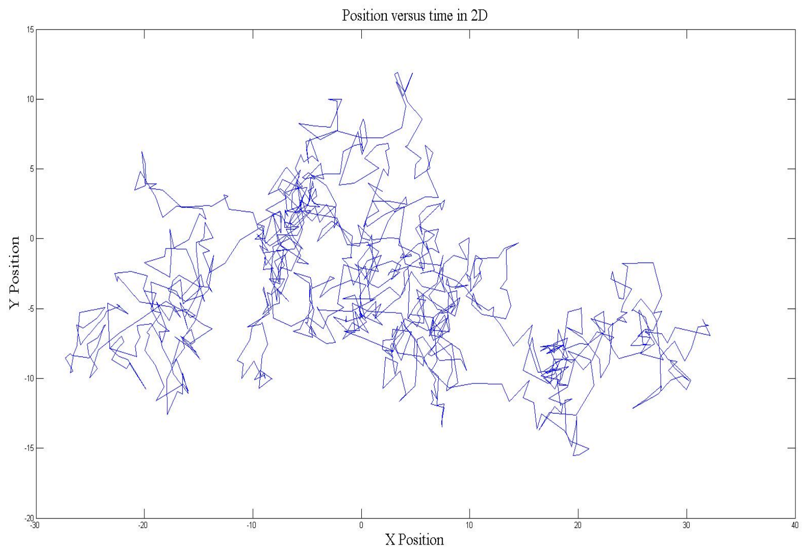

In 1905, using a probabilistic model, Albert Einstein provided an explanation of the Brownian motion [6]. Einstein's famous papers in 1905 have been reprinted numerous times (see a revision [29]). Later, Norbert Wiener constructed the following mathematical model for Brownian motion in the 1930s. For this reason the Brownian motion is also called Wiener process.

Definition 2.1.1 (Brownian motion, BM)**.** *A one-dimensional standard Brownian motion is a stochastic process $W = \{W_s, s \geqslant 0\}$ with following properties:*

(1) $W_0 = 0$, with probability 1.

(2) The function $s \to W_s$ is continuous in s with probability 1.

(3) The increment $W_{s+t} - W_s$ follows Gaussian distribution $N(0, t)$.

Figure 2.2: Graphs of five sample paths of Brownian motion.

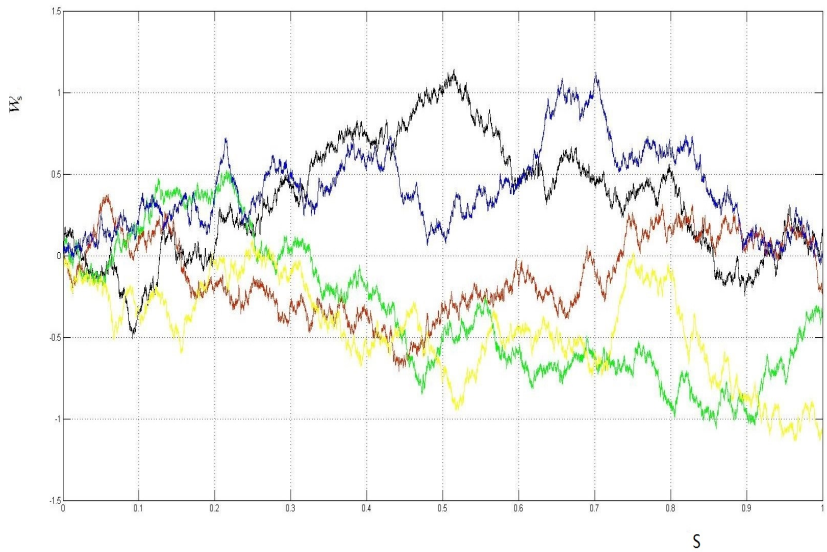

(4) The process W_s has independent increments.

A Brownian motion with initial value $W_0 = x$ is obtained by adding x to a standard Brownian motion. The term independent increments means that for every sequence of nonnegative real numbers $0 \leq t_1 \leq s_1 \leq t_2 \leq s_2 \leq \cdots \leq t_n \leq s_n < \infty$, the random variables

$$W_{s_1} - W_{t_1}, W_{s_2} - W_{t_2}, \cdots, W_{s_n} - W_{t_n}$$

are jointly independent.

The following lemma about BM will be frequently used in this thesis.

Lemma 2.1.2. *Let $t > 0$ be a finite time, and define the new process in $s \geq 0$ by*

$$\hat{W}_s = W_{t+s} - W_t.$$

Then $\hat{W} = \{\hat{W}_s, s \geqslant 0\}$ is a Brownian motion starting at 0 and independent of t.

This lemma is usually proved as a direct corollary of the strong Markovian property of Brownian motion [1, Section 37]. Here we present a proof by using the definition of Brownian motion.

Proof. We prove that $\hat{W}$ satisfies the four properties in Definition 2.1.1.

(1) $\hat{W}_0 = W_{t+0} - W_t = W_t - W_t = 0$.

(2) Since $t + s \to W_{t+s}$ is continuous in $t + s$ with probability 1 and $t \to W_t$ is continuous in t with probability 1, $W_{t+s} - W_t$ is continuous at s with probability 1, i.e., $s \to \hat{W}_s$ is continuous in s with probability 1.

(3) For any $u, v > 0$, $\hat{W}_{v+u} - \hat{W}_u = (W_{v+u+t} - W_t) - (W_{u+t} - W_t) = W_{v+u+t} - W_{u+t}$ follows the Gaussian distribution $N(0, v)$.

(4) For any nonnegative real numbers $0 \leq t_1 \leq s_1 \leq t_2 \leq s_2 \leq \cdots \leq t_n \leq s_n < \infty$ the increment random variables

$$\begin{aligned}
&\{\hat{W}_{s_1} - \hat{W}_{t_1}, \hat{W}_{s_2} - \hat{W}_{t_2}, \cdots, \hat{W}_{s_n} - \hat{W}_{t_n}\} \\
=&\{(W_{s_1+t} - W_t) - (W_{t_1+t} - W_t), (W_{s_2+t} - W_t) - (W_{t_2+t} - W_t), \\
&\cdots, (W_{s_n+t} - W_t) - (W_{t_n+t} - W_t)\} \\
=&\{W_{s_1+t} - W_{t_1+t}, W_{s_2+t} - W_{t_2+t}, \cdots, W_{s_n+t} - W_{t_n+t}\}
\end{aligned}$$

are jointly independent. $\square$

Definition 2.1.3 (Transition probability function)**.** *For a diffusion process $X = \{X_s, s \geq 0\}$, the transition probability function from the point y at time s to the point x at time $t > s$ is defined as*

$$p(x, t|y, s)\mathrm{d}x \triangleq P(X_t \in \mathrm{d}x | X_s = y).$$

The evolution of a diffusion process is governed by its transition probability function. Following directly from the properties (3) and (4) in Definition 2.1.1 we can obtain the transition probability function of Brownian motion which is called the Gauss kernel or sometimes the heat kernel.

Lemma 2.1.4 (Gauss kernel). *The transition probability function of Brownian motion from point y at time s to point x at time $t > s$ is*

$$p(x, t|y, s) = \frac{1}{\sqrt{2\pi(t-s)}} \exp\big[-\frac{(y-x)^2}{2(t-s)}\big].$$

It is well-known that the Gauss kernel satisfies the heat equation

$$\frac{\partial p}{\partial t} = \frac{1}{2}\frac{\partial^2 p}{\partial x^2}. \tag{2.1}$$

For the detailed probabilistic connections between Brownian motion and the heat equation, see [19]. In fact, this equation is a special case of the Fokker-Planck equation for duffussion processes [9]. The Fokker-Planck equation, also known as Kolmogorov forward equation, is satisfied under different boundary conditions, such as natural boundary conditions (upper boundary $+\infty$ and lower boundary $-\infty$), reflecting boundary conditions or absorbing boundary conditions. Specifically in this thesis, the heat equation (2.1) holds under absorbing boundary conditions.

Daniels [5] provided the following useful results concerning the FPD of Brownian motion.

Lemma 2.1.5. *Let $p^*(x, t)$ be the transition probability function of Brownian motion at point x and time t from point 0 at time 0, while not crossing the boudanry $c(s)$*

before time t. Then $p^*(x,t)$ satisfies the Fokker-Planck equation and the boundary condition $p^*(c(t),t) = 0$. Further, the BNCP is given by

$$P_W(t;c) = \int_{-\infty}^{c(t)} p^*(x,t)\mathrm{d}x, \tag{2.2}$$

and the first passage time density is given by

$$g_W(t;c) = -\frac{1}{2}\frac{\partial p^*(x,t)}{\partial x}\bigg|_{x\uparrow c(t)}. \tag{2.3}$$

Proof. We adopt the proof of Daniels [5] using the Fokker-Planck equation. By definition, we have

$$\begin{aligned}
\frac{\partial P_W(t;c)}{\partial t} &= \frac{\partial}{\partial t}\int_{-\infty}^{c(t)} p^*(x,t)\mathrm{d}x \\
&= p^*(c(t),t)\frac{\mathrm{d}}{\mathrm{d}t}c(t) + \int_{-\infty}^{c(t)} \frac{\partial p^*(x,t)}{\partial t}\mathrm{d}x \\
&= \frac{1}{2}\int_{-\infty}^{c(t)} \frac{\partial^2 p^*(x,t)}{\partial x^2}\mathrm{d}x \\
&= \frac{1}{2}\frac{\partial p^*(x,t)}{\partial x}\bigg|_{x\uparrow c(t)},
\end{aligned}$$

where the third equality holds because $p^*(c(t),t) = 0$ and $p^*(x,t)$ satisfies the heat equation (2.1). Therefore we have

$$g_W(t;c) = -\frac{\partial P_W(t;c)}{\partial t} = -\frac{1}{2}\frac{\partial p^*(x,t)}{\partial x}\bigg|_{x\uparrow c(t)}.$$

□

In the rest of this chapter, we derive the BNCP and FPD for Brownian motion and various boundaries.

2.2 Linear Boundary

We start by considering the linear boundary $c(s) = as + b$ where $s \geq 0$ and $b > 0$. Firstly, we introduce the well-known result of Siegmund [28] for the BNCP.

Lemma 2.2.1. *For the linear boundary $c(s) = as + b, s \geq 0,\ b > 0$ and any fixed t, the conditional probability of Brownian motion W not crossing the boundary $c(s)$ is given by*

$$\begin{aligned} &P(W_s < as + b, 0 \leq s < t | W_t = z) \\ =&\mathbb{1}_{\{z<at+b\}}\Big\{1 - \exp\big[-\frac{2b(at+b-z)}{t}\big]\Big\}. \end{aligned} \tag{2.4}$$

where $\mathbb{1}_{\{\cdot\}}$ is the indicator function.

Using the above formula, Wang and Poetzelberger [31] obtained the following result.

Corollary 2.2.2. *The BNCP $P_W(t;c)$ of Brownian motion for linear boundary $c(s) = as + b$, where $s \geq 0$ and $b > 0$, is*

$$P_W(t;c) = \Phi\big(\frac{at+b}{\sqrt{t}}\big) - \exp(-2ab)\Phi\big(\frac{at-b}{\sqrt{t}}\big). \tag{2.5}$$

Proof.

$$\begin{aligned} P_W(t;c) =&P(W_s < as + b, 0 \leq s \leq t) \\ =&\int_{-\infty}^{+\infty} P(W_s \leq as + b, 0 \leq s < t | W_t = z)\mathrm{d}P_t(z) \\ =&\int_{-\infty}^{at+b} \Big\{1 - \exp\big[-\frac{2b(at+b-z)}{t}\big]\Big\}\mathrm{d}P_t(z) \end{aligned}$$

$$=\Phi\big(\frac{at+b}{\sqrt{t}}\big)-\exp\big(-2ab\big)\Phi\big(\frac{at-b}{\sqrt{t}}\big),$$

where

$$\frac{\mathrm{d}P_t(z)}{\mathrm{d}z}=\frac{1}{\sqrt{2\pi t}}\exp\big(-\frac{z^2}{2t}\big)$$

is the probability density of W_t and $\Phi(\cdot)$ is the standard normal distribution function. $\square$

Corollary 2.2.3. *The FPD $g_W(t;c)$ for Brownian motion and linear boundary $c(s)=as+b, s\geq 0$ is given by*

$$g_W(t;c)=\frac{b}{2\sqrt{2\pi}t^{\frac{3}{2}}}\exp\big[-\frac{(at+b)^2}{2t}\big]. \tag{2.6}$$

Proof. By equation (1.1) and equation (2.5),

$$\begin{aligned} g_W(t;c)=&-\frac{\mathrm{d}}{\mathrm{d}t}P_W(t;c)\\ =&-\frac{\mathrm{d}}{\mathrm{d}t}\big[\Phi\big(\frac{at+b}{\sqrt{t}}\big)-\exp(-2ab)\Phi\big(\frac{at-b}{\sqrt{t}}\big)\big]\\ =&\frac{b}{2\sqrt{2\pi}t^{\frac{3}{2}}}\exp\big[-\frac{(at+b)^2}{2t}\big]. \end{aligned}$$

$\square$

The above well-known results for the BNCP and FPD and linear boundaries can be found in some textbooks on stochastic processes (e.g. [9, Chapter 4]).

2.3 Piecewise Linear Boundary

Now we consider piecewise linear boundaries that are linear on each of the finite subintervals of $[0, t]$.

Let $c(s)$ be a piecewise linear boundary on $[0, t]$ with nodes $(t_i)_{i=1}^n$, where $0 = t_0 < t_1 < \cdots < t_{n-1} < t_n = t, n > 1$, i.e., $c(s)$ is linear on each interval (t_{j-1}, t_j). Further, $c(s)$ is continuous at time 0 and time t with $c(0) > 0$.

Figure 2.3: A piecewise linear boundary.

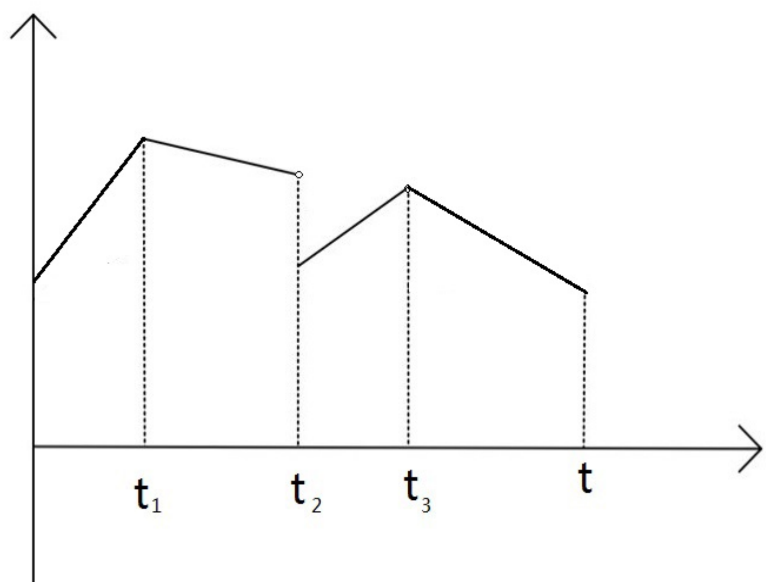

Denote $c_j^+ = \lim_{\Delta t \to 0+} c(t_j + \Delta t)$, $c_j^- = \lim_{\Delta t \to 0+} c(t_j - \Delta t), j = 1, 2, \cdots, n-1$ and $c_0^+ = c(0)$, $c_n^- = c(t)$. Let $\beta_j = \min\{c_j^+, c_j^-\}$, $j = 1, 2, \cdots, n-1$, $\beta_0 = c(0)$, $\beta_n = c(t)$. Note that the boundary can be discontinuous at node t_j.

2.3.1 Boundary Non-Crossing Probability

In this subsection, we give a closed-form formula for the BNCP and piecewise linear boundaries, which is the first main result of this thesis.

Theorem 2.3.1. *The BNCP $P_W(t;c)$ for the piecewise linear boundary $c(s)$ is given by*

$$P_W(t;c) = \int_{(\boldsymbol{-\infty},\boldsymbol{\beta_n})} \prod_{i=1}^{n} \Big\{ 1 - \exp\big[- \frac{2(c_{i-1}^{+} - x_{i-1})(c_i^{-} - x_i)}{t_i - t_{i-1}} \big] \Big\} f(\boldsymbol{x}) \mathrm{d}\boldsymbol{x}, \tag{2.7}$$

where $\boldsymbol{x} = (x_1, x_2, \cdots, x_n)$,

$$f(\boldsymbol{x}) = \prod_{i=1}^{n} \frac{1}{\sqrt{2\pi(t_i - t_{i-1})}} \exp\big[- \frac{(x_i - x_{i-1})^2}{2(t_i - t_{i-1})} \big],$$

and the region of integration is $\boldsymbol{(-\infty, \beta_n)} = (-\infty, \beta_1) \times (-\infty, \beta_2) \times \cdots \times (-\infty, \beta_n)$.

We prove the result using the method of Wang and Poetzelberger [31].

Proof. By Definition 2.1.1 of Brownian motion and the result of Lemma 2.1.2, we have

$$\begin{aligned} P_W(t;c) =& P(W_s < c(s), 0 \le s \le t) \\ &= \int_{-\infty}^{+\infty} \mathbb{1}_{\{x_1 < c_1^{-}\}} P(W_s < c(s), t_1 \ne s \le t | W_{t_1} = x_1) dP_{t_1}(x_1) \\ &= \int_{-\infty}^{+\infty} \mathbb{1}_{\{x_1 < c_1^{-}\}} P(W_s < c(s), 0 \le s < t_1 | W_{t_1} = x_1) \\ &\quad \times \mathbb{1}_{\{x_1 < c_1^{+}\}} P(W_s < c(s), t_1 < s \le t | W_{t_1} = x_1) \mathrm{d}P_{t_1}(x_1) \\ &= \int_{-\infty}^{+\infty} \mathbb{1}_{\{x_1 < \min(c_1^{-}, c_1^{+}) = \beta_1\}} P(W_s < c(s), 0 \le s < t_1 | W_{t_1} = x_1) \end{aligned}$$

$$\times P(W_s < c(s), t_1 < s \le t | W_{t_1} = x_1) \mathrm{d}P_{t_1}(x_1)$$

$$= \int_{-\infty}^{\beta_1} P(W_s < c(s), 0 \le s < t_1 | W_{t_1} = x_1)$$

$$\times P(W_s < c(s), t_1 < s \le t | W_{t_1} = x_1) \mathrm{d}P_{t_1}(x_1),$$

where by equation (2.4) the first factor in the last integral is

$$P(W_s < c(s), 0 \le s < t_1 | W_{t_1} = x_1) = 1 - \exp\big[- \frac{2c_0^+(c_1^- - x_1)}{t_1} \big].$$

Further, the second factor in the last integral is

$$P(W_s < c(s), t_1 < s \le t | W_{t_1} = x_1)$$

$$= P(W_s < c(s + t_1) - x_1, s \le t - t_1)$$

$$= \int_{-\infty}^{+\infty} \mathbb{1}_{\{x_2 < (c_2^- - x_1)\}} \left\{ 1 - \exp\big[- \frac{2(c_1^+ - x_1)(c_2^- - x_1 - x_2)}{t_2 - t_1} \big] \right\} \mathbb{1}_{\{x_2 < (c_2^+ - x_1)\}}$$

$$P(W_s < c(s + t_1) - x_1, t_2 - t_1 < s \le t - t_1 | W_{t_2 - t_1} = x_2) \mathrm{d}P_{t_2 - t_1}(x_2)$$

$$= \int_{-\infty}^{+\infty} \mathbb{1}_{\{x_2 < c_2^-\}} \left\{ 1 - \exp\big[- \frac{2(c_1^+ - x_1)(c_2^- - x_2)}{t_2 - t_1} \big] \right\} \mathbb{1}_{\{x_2 < c_2^+\}}$$

$$P(W_s < c(s + t_1) - x_1, t_2 - t_1 < s \le t - t_1 | W_{t_2 - t_1} = x_2 - x_1) \mathrm{d}P_{t_2 - t_1}(x_2 - x_1)$$

$$= \int_{-\infty}^{+\infty} \mathbb{1}_{\{x_2 < \min(c_2^-, c_2^+) = \beta_2\}} \left\{ 1 - \exp\big[- \frac{2(c_1^+ - x_1)(c_2^- - x_2)}{t_2 - t_1} \big] \right\}$$

$$P(W_s < c(s + t_2) - x_2, s \le t - t_2) \mathrm{d}P_{t_2 - t_1}(x_2 - x_1)$$

$$= \int_{-\infty}^{\beta_2} \left\{ 1 - \exp\big[- \frac{2(c_1^+ - x_1)(c_2^- - x_2)}{t_2 - t_1} \big] \right\}$$

$$P(W_s < c(s + t_2) - x_2, s \le t - t_2) \mathrm{d}P_{t_2 - t_1}(x_2 - x_1).$$

Apply the same calculation to $P(W_s < c(s+t_2) - x_2, s \le t - t_2)$ and repeat the steps until we get

$$
\begin{aligned}
& P(W_s < c(s+t_{n-1}) - x_{n-1}, s \le t - t_{n-1}) \\
= & \int_{-\infty}^{\beta_n} \Big\{ 1 - \exp\big[- \frac{2(c_{n-1}^{+} - x_{n-1})(c_n^{-} - x_n)}{t - t_{n-1}} \big] \Big\} \mathrm{d}P_{t-t_{n-1}}(x_n - x_{n-1}).
\end{aligned}
$$

The result follows by combining all the above steps. $\square$

In the following, we give another proof of this theorem.

A second proof. Define the events

$$A_i = \{W_s < c(s), t_{i-1} < s < t_i | W_{t_{i-1}} = x_{i-1}, W_{t_i} = x_i\}, i = 1, 2, \cdots, n.$$

Figure 2.4: A sample path that does not cross the boundary before t.

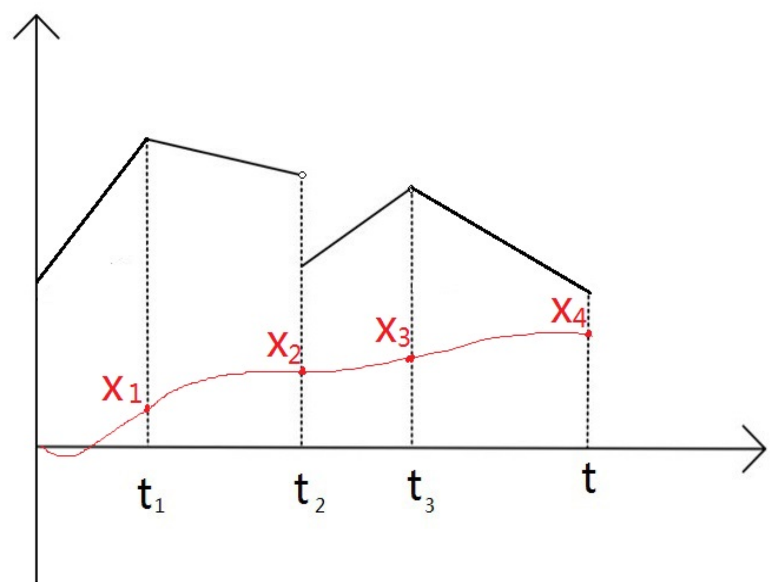

By the property of BM, $\{A_i\}$ are independent of each other. Therefore

$$P(W_s < c(s), 0 \le s < t, s \ne t_j | W_{t_1} = x_1, W_{t_2} = x_2, \ldots, W_{t_n} = x_n)$$

$$= P(A_1 \cap A_2 \cap \cdots \cap A_n) = \prod_{i=1}^{n} P(A_i),$$

where

$$P(A_i) = \mathbb{1}_{\{x_{i-1} < c_{i-1}^{+}\}} \mathbb{1}_{\{x_i < c_i^{-}\}} \left\{ 1 - \exp\Big[-\frac{2(c_{i-1}^{+} - x_{i-1})(c_i^{-} - x_i)}{t_i - t_{i-1}} \Big] \right\}.$$

Since $f(\boldsymbol{x})$ is the joint density function of $W_{t_1}, W_{t_2}, \cdots, W_{t_n}$, we have

$$P(W_s < c(s), 0 \le s \le t)$$

$$= \int P(W_s < c(s), 0 \le s < t, s \ne t_j | W_{t_1} = x_1, W_{t_2} = x_2, \ldots, W_{t_n} = x_n) f(\boldsymbol{x}) \mathrm{d}\boldsymbol{x}$$

$$= \int \prod_{i=1}^{n} P(A_i) f(\boldsymbol{x}) \mathrm{d}\boldsymbol{x}$$

$$= \int \prod_{i=1}^{n} \mathbb{1}_{\{x_i < \beta_i\}} \left\{ 1 - \exp\Big[-\frac{2(c_{i-1}^{+} - x_{i-1})(c_i^{-} - x_i)}{t_i - t_{i-1}} \Big] \right\} f(\boldsymbol{x}) \mathrm{d}\boldsymbol{x}$$

$$= \int_{(-\boldsymbol{\infty}, \boldsymbol{\beta_n})} \prod_{i=1}^{n} \left\{ 1 - \exp\Big[-\frac{2(c_{i-1}^{+} - x_{i-1})(c_i^{-} - x_i)}{t_i - t_{i-1}} \Big] \right\} f(\boldsymbol{x}) \mathrm{d}\boldsymbol{x}.$$

□

Now let us consider a special case where the piecewise linear boundary is continuous. In this case $\beta_j = c_j^{+} = c_j^{-} = c(t_j)$ for every j. Further, let $c_j = c(t_j)$. Then Theorem 2.3.1 implies the following result given by Wang and Poetzelberger [31].

Corollary 2.3.2. *The BNCP $P_W(t;c)$ for continuous piecewise linear boundary $c(s)$ is given by*

$$P_W(t;c) = \int_{(-\infty, c_n)} \prod_{i=1}^{n} \left\{ 1 - \exp\left[-\frac{2(c_{i-1} - x_{i-1})(c_i - x_i)}{t_i - t_{i-1}} \right] \right\} f(\boldsymbol{x}) \mathrm{d}\boldsymbol{x},$$

where

$$f(\boldsymbol{x}) = \prod_{i=1}^{n} \frac{1}{\sqrt{2\pi(t_i - t_{i-1})}} \exp\left[-\frac{(x_i - x_{i-1})^2}{2(t_i - t_{i-1})} \right]$$

and the region of integration is $\boldsymbol{(-\infty, c_n)} = (-\infty, c_1) \times (-\infty, c_2) \times \cdots \times (-\infty, c_n)$.

2.3.2 First Passage Time Density

In this subsection, we present the second main result in this thesis.

Theorem 2.3.3. *Let $c(s)$ be the piecewise linear boundary defined on the partition $0 = t_0 < t_1 < \cdots < t_{n-1} < t_n$. For any $1 < m \leq n$ and $t_{m-1} < t < t_m$, the FPD is given by*

$$\begin{aligned} g_W(t;c) = & \int_{(-\infty, \beta_{m-1})} \prod_{i=1}^{m-1} \left\{ 1 - \exp\left[-\frac{2(c_{i-1}^{+} - x_{i-1})(c_i^{-} - x_i)}{t_i - t_{i-1}} \right] \right\} \\ & \times \frac{c_{m-1}^{+} - x_{m-1}}{\sqrt{2\pi}(t - t_{m-1})^{\frac{3}{2}}} \exp\left[-\frac{(c(t) - x_{m-1})^2}{2(t - t_{m-1})} \right] f(\boldsymbol{x}) \mathrm{d}\boldsymbol{x}, \end{aligned} \tag{2.8}$$

where $\boldsymbol{x} = (x_1, x_2, \cdots, x_{m-1})$.

Proof. By expanding the inner integral of (2.7), we have

$$P_W(t;c)$$

$$= \int_{-\infty}^{c(t)} \int_{(-\infty, \beta_{m-1})} \prod_{i=1}^{m-1} \left\{ 1 - \exp\left[- \frac{2(c_{i-1}^{+} - x_{i-1})(c_i^{-} - x_i)}{t_i - t_{i-1}} \right] \right\} f(\boldsymbol{x})$$

$$\times \left\{ 1 - \exp\left[- \frac{2(c_{m-1}^{+} - x_{m-1})(c(t) - x)}{t - t_{m-1}} \right] \right\} \frac{\exp[-\frac{(x - x_{m-1})^2}{2(t - t_{m-1})}]}{\sqrt{2\pi(t - t_{m-1})}} \mathrm{d}\boldsymbol{x} \mathrm{d}x$$

$$= \int_{-\infty}^{c(t)} p^*(x, t) \mathrm{d}x,$$

where

$$p^*(x, t) = \int_{(-\infty, \beta_{m-1})} \prod_{i=1}^{m-1} \left\{ 1 - \exp\left[- \frac{2(c_{i-1}^{+} - x_{i-1})(c_i^{-} - x_i)}{t_i - t_{i-1}} \right] \right\} f(\boldsymbol{x})$$

$$\times \left\{ 1 - \exp\left[- \frac{2(c_{m-1}^{+} - x_{m-1})(c(t) - x)}{t - t_{m-1}} \right] \right\} \frac{\exp[-\frac{(x - x_{m-1})^2}{2(t - t_{m-1})}]}{\sqrt{2\pi(t - t_{m-1})}} \mathrm{d}\boldsymbol{x}$$

satisfies conditions given in Lemma 2.1.5.

Denote the part that depends on x and t by

$$\gamma(x, t) = \left\{ 1 - \exp\left[- \frac{2(c_{m-1}^{+} - x_{m-1})(c(t) - x)}{t - t_{m-1}} \right] \right\} \frac{\exp[-\frac{(x - x_{m-1})^2}{2(t - t_{m-1})}]}{\sqrt{2\pi(t - t_{m-1})}}.$$

Then,

$$\frac{\partial \gamma(x, t)}{\partial x}$$

$$= - \frac{x - x_{m-1}}{t - t_{m-1}} \left\{ 1 - \exp\left[- \frac{2(c_{m-1}^{+} - x_{m-1})(c(t) - x)}{t - t_{m-1}} \right] \right\} \frac{\exp[-\frac{(x - x_{m-1})^2}{2(t - t_{m-1})}]}{\sqrt{2\pi(t - t_{m-1})}}$$

$$- \frac{\exp[-\frac{(x - x_{m-1})^2}{2(t - t_{m-1})}]}{\sqrt{2\pi(t - t_{m-1})}} \exp\left[- \frac{2(c_{m-1}^{+} - x_{m-1})(c(t) - x)}{t - t_{m-1}} \right] \frac{2(c_{m-1}^{+} - x_{m-1})}{t - t_{m-1}}.$$

Since

$$1-\exp\big[-\frac{2(c_{m-1}^{+}-x_{m-1})(c(t)-x)}{t-t_{m-1}}\big]\Big|_{x\uparrow c(t)}=0$$

and

$$\Big|\frac{x-x_{m-1}}{t-t_{m-1}}\frac{\exp[-\frac{(x-x_{m-1})^2}{2(t-t_{m-1})}]}{\sqrt{2\pi(t-t_{m-1})}}\Big|\Big|_{x\uparrow c(t)}$$

is bounded, we have

$$\frac{\partial\gamma(x,t)}{\partial x}\big|_{x\uparrow c(t)}=-\frac{2(c_{m-1}^{+}-x_{m-1})}{\sqrt{2\pi}(t-t_{m-1})^{\frac{3}{2}}}\exp\big[-\frac{(c(t)-x_{m-1})^2}{2(t-t_{m-1})}\big].$$

Therefore by Lemma 2.1.5, we have

$$g_W(t;c)=-\frac{1}{2}\frac{\partial p^*(x,t)}{\partial x}\Big|_{x\uparrow c(t)}$$

$$=\int_{(-\boldsymbol{\infty},\boldsymbol{\beta_{m-1}})}\prod_{i=1}^{m-1}\Big\{1-\exp\big[-\frac{2(c_{i-1}^{+}-x_{i-1})(c_i^{-}-x_i)}{t_i-t_{i-1}}\big]\Big\}$$

$$\times\big[-\frac{1}{2}\frac{\partial\gamma(x,t)}{\partial x}\Big|_{x\uparrow c(t)}\big]f(\boldsymbol{x})\mathrm{d}\boldsymbol{x}$$

$$=\int_{(-\boldsymbol{\infty},\boldsymbol{\beta_{m-1}})}\prod_{i=1}^{m-1}\Big\{1-\exp\big[-\frac{2(c_{i-1}^{+}-x_{i-1})(c_i^{-}-x_i)}{t_i-t_{i-1}}\big]\Big\}$$

$$\times\frac{c_{m-1}^{+}-x_{m-1}}{\sqrt{2\pi}(t-t_{m-1})^{\frac{3}{2}}}\exp\big[-\frac{(c(t)-x_{m-1})^2}{2(t-t_{m-1})}\big]f(\boldsymbol{x})\mathrm{d}\boldsymbol{x}.$$

□

From equation (2.8) we can see a very interesting property of the FPD.

Corollary 2.3.4. *Suppose two piecewise linear boundaries $h(s)$ and $l(s)$ with the same nodes $0 = t_0 < t_1 < \cdots < t_m < t_{m+1} < \cdots$ such that $h(s) \geq l(s)$, $\forall 0 \leq s \leq t$ and $h(s) > l(s)$ for s in at least on subinterval $[t_{i-1}, t_i]$ $1 \leq i \leq m$, and $h(t) = l(t)$, $t \in (t_m, t_{m+1})$. Let $g_W(t; h)$ and $g_W(t; l)$ be the FPD for $h(s)$ and $l(s)$ at time t respectively. Then $g_W(t; h) > g_W(t; l)$.*

Figure 2.5: $g_W(t; h) > g_W(t; l)$.

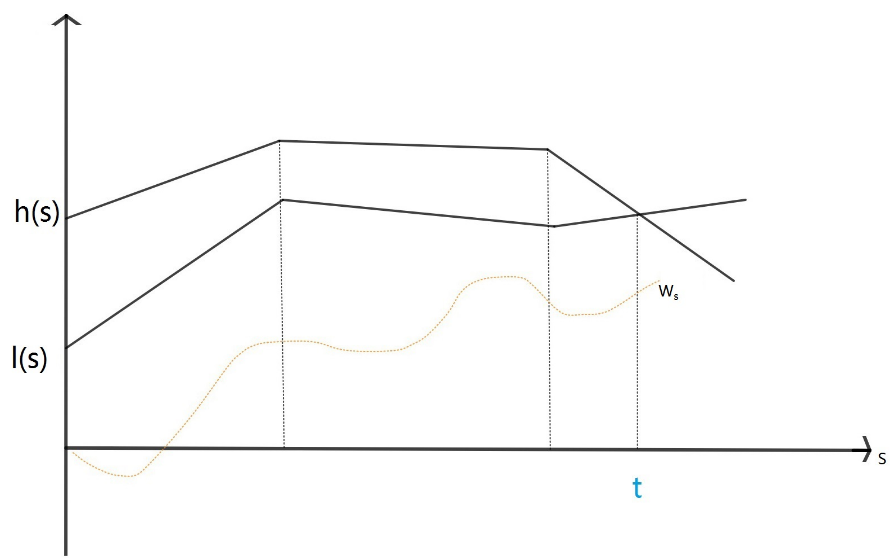

Proof. It is easy to see that $g(t; \cdot)$ in equation (2.8) is an increasing function of c_j^+ and c_j^-, $i = 1, 2, \cdots, m$. $\square$

The above corollary is interesting and somewhat surprising. While it is easy to understand that the boundary non-crossing probability is greater for higher boundary, it does not necessarily imply greater density. The following example helps us to understand this point.

Figure 2.6: Graph for Example 2.3.6.

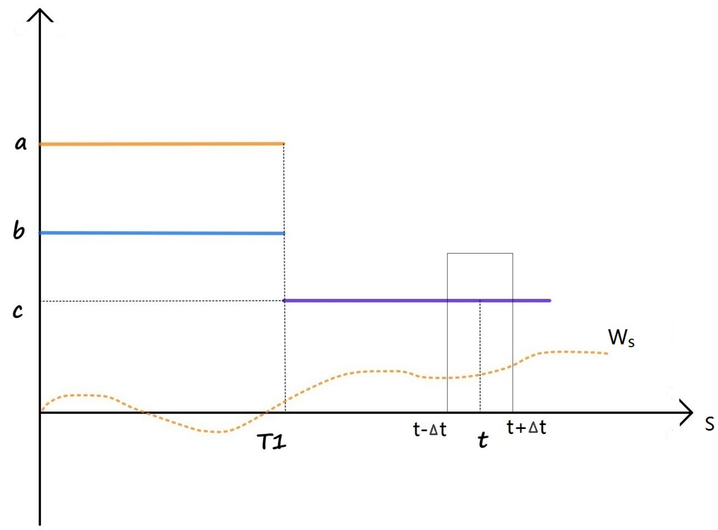

.

Example 2.3.5. Let $h(s) = a, 0 \leq s \leq T_1$ and $h(s) = c, s > T_1$; $l(s) = b, 0 \leq s \leq T_1$ and $l(s) = c, s > T_1$, where $a > b > c > 0$. Then for any $t > T_1$,

$$P(W_s < h(s), 0 \leq s \leq t)$$

$$= \int_{-\infty}^{c} P(W_s < a, 0 \leq t \leq T_1 | W_{T_1} = x) P(W_s < c - x, 0 < s \leq t - T_1) \mathrm{d}x.$$

Therefore,

$$g_W(t; h) = -\frac{\partial}{\partial t} P(W_s < h(s), 0 \leq s \leq t))$$

$$= -\int_{-\infty}^{c} P(W_s < a, 0 \leq s \leq T_1 | W_{T_1} = x) \frac{\partial}{\partial t} P(W_s < c - x, 0 < s \leq t - T_1) \mathrm{d}x.$$

Similarly we have for $t > T_1$,

$$g_W(t; l) = -\frac{\partial}{\partial t} P(W_s < l(s), 0 \leq s \leq t))$$

$$= -\int_{-\infty}^{c} P(W_s < b, 0 \leq s \leq T_1 | W_{T_1} = x) \frac{\partial}{\partial t} P(W_s < c - x, 0 < s \leq t - T_1) \mathrm{d}x.$$

For any $x < c$,

$$P(W_s < b, 0 \leq t \leq T_1 | W_{T_1} = x) < P(W_s < a, 0 \leq s \leq T_1 | W_{T_1} = x).$$

It follows that $g_W(t; l) < g_W(t; h)$.

Now we give an experimental explanation. Take Brown's example in his 1827 report of N yellow pollen particles under a microscope. The displacement of each particle along a fixed axis can be regarded as a standard Brownian motion. Let $0 < T_1 < T$ be fixed. If a particle does not reach $h(s) = h$ before T_1, then it is said to be in class 1. If a particle does not reach $l(s) = b$ before T_1, then it belongs to class 2. If, after T_1, a particle reaches c in a small interval $(t - \frac{1}{2}\Delta t, t + \frac{1}{2}\Delta t)$, then it is said to be in class A. Then it is clear that the number N_1 of particles in both class 1 and A is greater than or equal to the number N_2 of particles in both class 2 and A, so that $N_1/N \geq N_2/N$. For sufficiently large N and small Δt, N_1/N and N_2/N can be regarded as the FPD values under upper and lower boundaries respectively.

Similar to the BNCP, the FPD result can be simplified for continuous piecewise linear boundary where $\beta_j = c_j^+ = c_j^- = c(t_j) = c_j$.

Corollary 2.3.6. *If $c(s)$ is continuous piecewise linear boundary, then the first passage time density $g_W(t; c)$ on $t_{m-1} < t < t_m$ is given by*

$$\begin{aligned} g_W(t; c) = \int_{(-\infty, \boldsymbol{c}_{m-1})} \prod_{i=1}^{m-1} \Big\{ 1 - \exp\big[-\frac{2(c_{i-1} - x_{i-1})(c_i - x_i)}{t_i - t_{i-1}} \big] \Big\} \\ \times \frac{c_{m-1} - x_{m-1}}{\sqrt{2\pi}(t - t_{m-1})^{\frac{3}{2}}} \exp\big[-\frac{(c(t) - x_{m-1})^2}{2(t - t_{m-1})} \big] f(\boldsymbol{x}) \mathrm{d}\boldsymbol{x}, \end{aligned} \tag{2.9}$$

where $\boldsymbol{x} = (x_1, x_2, \cdots, x_{m-1})$ *and the region of integration is* $(\boldsymbol{-\infty, c_{m-1}}) = (-\infty, c_1) \times (-\infty, c_2) \times \cdots \times (-\infty, c_{m-1})$.

Sometimes researchers are interested in the conditional BNCP given that the process ends at a particular point. This conditional probability is also useful in the computation of BNCP for general boundaries as shown later.

Theorem 2.3.7. *Let* $c(s)$ *be a piecewise linear boundary on* $[0, t]$ *with nodes* $(t_i)_{i=1}^{n}$, *where* $0 = t_0 < t_1 < \cdots < t_{n-1} < t_n = t, n > 1$. *Given* $W_t = x$, *the conditional BNCP is*

$$\begin{aligned}
&P_W(t; c|W_t = x)\\
=&P(W_s < c(s), 0 \leq s < t|W_t = x)\\
=&\mathbb{1}_{\{x<c(t)\}} \int_{(-\infty, \boldsymbol{\beta}_{(n-1)\times 1})} \prod_{i=1}^{n-1} \left(1 - \exp(-\frac{2(c_{i-1}^{+} - x_{i-1})(c_i^{-} - x_i)}{t_i - t_{i-1}})\right)\\
&\times \left(1 - \exp(-\frac{2(c_{n-1}^{+} - x_{n-1})(c(t) - x)}{T - t_{n-1}})\right)\\
&\times \frac{\sqrt{t}}{\sqrt{t - t_{n-1}}} \exp(-\frac{t x_{n-1}^2 - 2x x_{n-1} + t_{n-1} x^2}{2t(t - t_{n-1})}) f(\boldsymbol{x}) \mathrm{d}\boldsymbol{x},
\end{aligned} \tag{2.10}$$

where $\boldsymbol{x} = (x_1, x_2, \cdots, x_{n-1})$.

Proof. To simplify notation, we denote the transition probability function of BM at point x and time $t > 0$ from point 0 at time 0 as

$$p(x, t) = p(x, t|0, 0) = \frac{1}{\sqrt{2\pi t}} \exp(-\frac{x^2}{2t}).$$

Then by the definition of conditional probability,

$$P(\tau_c \geq t | W_t = x) = \frac{p^*(x,t)}{p(x,t)}, \tag{2.11}$$

where in the proof of Theorem 2.3.1 we have obtained

$$p^*(x,t) = \int_{(-\infty,\boldsymbol{\beta}_{n-1})} \prod_{i=1}^{n-1} \left\{1 - \exp\left[-\frac{2(c_{i-1}^+ - x_{i-1})(c_i^- - x_i)}{t_i - t_{i-1}}\right]\right\} f(\boldsymbol{x})$$

$$\times \left\{1 - \exp\left[-\frac{2(c_{n-1}^+ - x_{n-1})(c(t) - x)}{t - t_{n-1}}\right]\right\} \frac{\exp[-\frac{(x-x_{n-1})^2}{2(t-t_{n-1})}]}{\sqrt{2\pi(t-t_{n-1})}} \mathrm{d}\boldsymbol{x}.$$

□

2.4 General Boundary

In previous sections we have derived explicit formulas of the BNCP and FPD for piecewise linear boundaries. In this section we use these formulas to obtain approximations for the BNCP and FPD for general boundaries.

Firstly, we consider concave boundaries as shown in Figure 2.7.

Figure 2.7: A concave boundary.

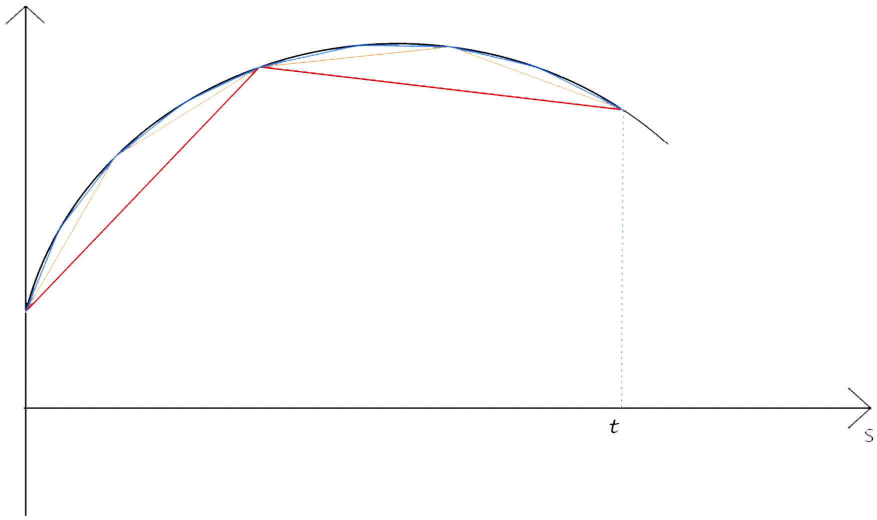

Lemma 2.4.1 (BNCP of a concave boundary)**.** *Let boundary $c(s)$ be a concave differentiable function on $[0,t]$ and time interval $[0,t]$ is partitioned into $n = 2^k$ equal-length subintervals ($k > 1$) with nodes $0 = t_0 < t_1 < \cdots < t_{2^k-1} < t_{2^k} = t$. Denote by $c_k(s)$ the polygonal function connecting points $c_j = c(t_j), j = 0, 1, \cdots, 2^k$. Then $P(t; c) = \lim_{k\to\infty} P(t; c_k)$.*

Proof. Define events $A_k = \{W_s < c_k(s), 0 < s \leq t\}$ and $A = \{W_s < c(s), 0 < s \leq t\}$. Since $c(s)$ is concave on $[0,t]$, we have $c_{k+1}(s) \geq c_k(s)$, $\forall s \in [0,t]$, and hence $A_k \subset A_{k+1}$. Further, by definition $c_k(s)$ converge to $c(s)$ uniformly on $[0,t]$. Therefore, $\bigcup_{k=1}^{\infty} A_k = A$. By the continuity property of the probability measure, $P(A) = \lim_{k\to\infty} P(A_k)$, i.e.,

$$P(W_s < c(s), 0 \leq s \leq t) = \lim_{k\to\infty} P(W_s < c_k(s), 0 \leq s \leq t).$$

□

Now we continue to consider the FPD at t.

Lemma 2.4.2. *Let $c(s)$ be continuously differentiable and concave on $(0, +\infty)$. For a fixed $t > 0$, partition $[0, t]$ into 2^k $(k \geq 1)$ equal-length intervals with nodes $0 = t_0 < t_1 < \cdots < t_{2^k-1} < t_{2^k} = t$. Let $c_k(s)$ be the polygonal function taking points $c_j = c(t_j), j = 0, 1, \cdots, 2^k$ as vertices on $0 < s \leq t$, and be continuously differentiable at t. Then $\lim_{k\to\infty} g_W(t; c_k)$ exists.*

Figure 2.8: Piecewise linear boundaries $c_k(s)$ for a concave boundary $c(s)$.

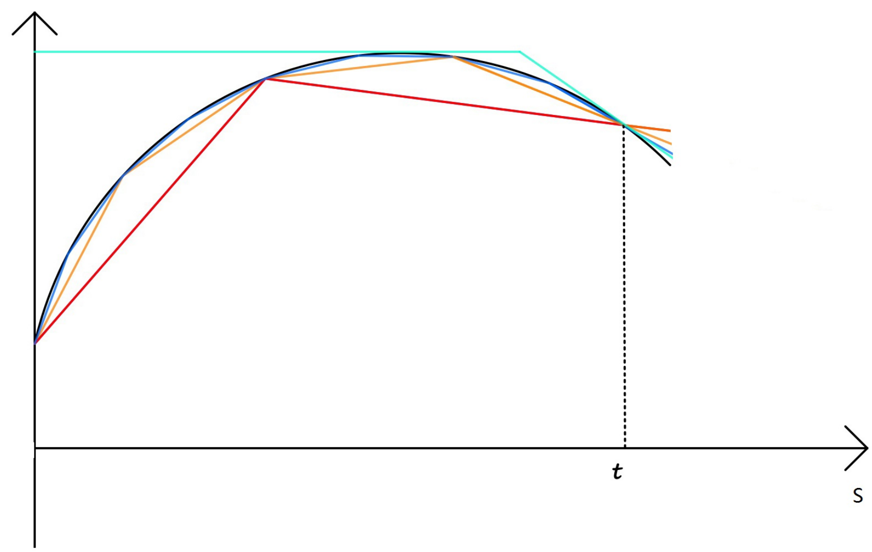

Proof. Since $c(s)$ is concave, we have $c_{k+1}(s) > c_k(s)$, $0 < s < t$ except for some nodes where $c_{k+1}(t_j) = c_k(t_j)$. Therefore by Corollary 2.3.4, we have $g_W(t; c_{k+1}) > g_W(t; c_k)$.

Further, we can always find a boundary $b(s)$ (the green boundary in Figure 2.6) such that $b(s) > c_k(s)$, $0 < s < t$ and $b(t) = c_k(t)$ for all k. Then by Corollary 2.3.4

we have $g_W(t;c_k) < g_W(t;b)$, i.e., $g_W(t;c_k)$ are uniformly bounded.

Since $g_W(t;c_k)$ are bounded and monotone increasing, $\lim_{k\to\infty} g_W(t;c_k)$ exists. $\square$

Note that the piecewise linear boundaries $c_k(s)$ approximate the differentiable concave $c(s)$ from below. Similarly, we can construct a sequence of piecewise linear boundaries that approximate $c(s)$ from above. Let $h_k(s)$ be the piecewise linear function consisting of the tangent lines at (t_j, c_j) (the green boundaries in Figure 2.7). Then $h_k(s)$ converge uniformly to $c(s)$. Since $c(s)$ is concave, $h_k(s) \geq c(s)$, $\forall k$ and $h_{k+1}(s) \leq h_k(s)$. Therefore similar to the BNCP and FPD for $c_k(s)$, it follows that $P(t;c) = \lim_{k\to\infty} P(t;h_k)$ and $\lim_{k\to\infty} g_W(t;h_k)$ exists.

Figure 2.9: Upper and lower boundary of a concave boundary.

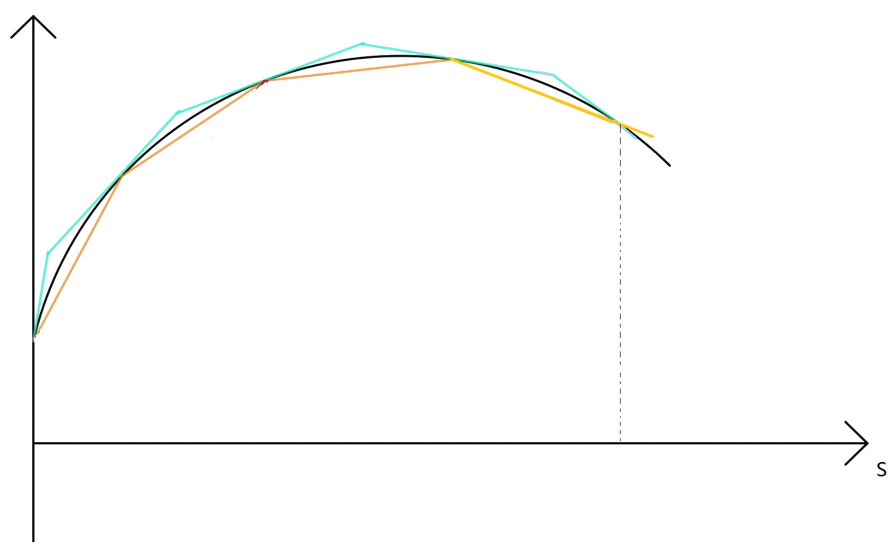

For the BNCP for general boundaries, Wang and Poetzelberger [31] provided the following result

Lemma 2.4.3. *If $c_n^*(s) \to c(s)$ as $n \to \infty$ uniformly on $[0, t]$, then,*

$$P(W_s < c(s), 0 < s < t) = \lim_{n\to\infty} P(W_s < c_n^*(s), 0 < s < t)).$$

It is easy to see that the case of convex boundaries can be dealt with similarly. Moreover, the partition of interval $[0, t]$ does not have to be equally spaced. In general, we can always separate the boundary into convex and concave parts and use the above method to define the upper and lower boundaries respectively.

Chapter 3

Computational Algorithms and Numerical Examples

In this Chapter, we develop numerical algorithms to compute the BNCP and FPD by Monte Carlo method. One advantage of this approach is that the accuracy of approximation can be assessed through the standard procedures of Monte Carlo simulation, especially when the boundary is piecewise linear. In addition, numerical examples are provided to illustrate the simulation method.

3.1 Boundary Non-Crossing Probability

For piecewise linear boundaries, equation (2.7) in Theorem 2.3.1 can be expressed as

$$P_W(t;c) = \mathrm{E}[v(W_{t_1}, W_{t_2}, \cdots, W_{t_n})], \tag{3.1}$$

where $v(\cdot)$ is given by

$$v(x_1, x_2, \cdots, x_n) = \prod_{i=1}^{n} \mathbb{1}_{\{x_i < \beta_i\}} \left\{ 1 - \exp\left[- \frac{2(c_{i-1}^{+} - x_{i-1})(c_i^{-} - x_i)}{t_i - t_{i-1}} \right] \right\}. \tag{3.2}$$

Hence $P_W(t;c)$ can be estimated by $\hat{J} = \sum_{j=1}^{N} v(\boldsymbol{x}^j)/N$, where $\boldsymbol{x}^j = (x_1^j, x_2^j, \cdots, x_n^j)$, $j = 1, 2, \cdots, N$, are random samples drawn from the joint distribution of $W_{t_1}, W_{t_2}, \cdots, W_{t_n}$. By the law of large numbers, the estimator $\sum_{j=1}^{N} v(\boldsymbol{x}^j)/N$ converges in probability to $P_W(t;c)$ as $N \to \infty$.

Note that the increments are jointly independent and $W_{t_i} - W_{t_{i-1}}$ follows the Gaussian distribution $N(0, t_i - t_{i-1})$. We firstly generate i.i.d sample $\boldsymbol{u} = (u_1, u_2, \cdots, u_n)$ from the standard Normal distribution $N(0,1)$. Then we can obtain a sample $\boldsymbol{x} = (x_1, x_2, \cdots, x_n)$ of $(W_{t_1}, W_{t_2}, \cdots, W_{t_n})$ by transformation $\boldsymbol{x} = MD^{1/2}\boldsymbol{u}$, where $D^{1/2} = diag(\sqrt{t_1 - t_0}, \sqrt{t_2 - t_1}, \cdots, \sqrt{t_n - t_{n-1}})$ and

$$M = \begin{pmatrix} 1 & 0 & \cdots & 0 \\ 1 & 1 & & \vdots \\ \vdots & & \ddots & \vdots \\ 1 & \cdots & \cdots & 1 \end{pmatrix},$$

i.e., $x_i = u_1\sqrt{t_1 - t_0} + u_2\sqrt{t_2 - t_1} + \cdots + u_i\sqrt{t_i - t_{i-1}}$, $i = 1, 2, \cdots, n$.

The computational algorithm to calculate the BNCP is as following.

(1) Generate an i.i.d sample $\boldsymbol{u} = (u_1, u_2, \cdots, u_n)$ from the standard Normal distribution $N(0,1)$.

(2) Compute $\boldsymbol{x} = (x_1, x_2, \cdots, x_n)$ by $\boldsymbol{x} = MD^{1/2}\boldsymbol{u}$.

(3) Calculate the values of $(c_1^+, c_2^+, \cdots, c_n^+)$, $(c_1^-, c_2^-, \cdots, c_n^-)$ and $(\beta_1, \beta_2, \cdots, \beta_n)$ where $\beta_i = \min\{c_i^+, c_i^-\}$ for the boundary.

(4) Calculate $v(\boldsymbol{x})$ by equation (3.2).

(5) Repeat steps (1)-(4) N times and then calculate the estimate $\hat{J}(t;c) = \sum v(\boldsymbol{x})/N$.

The BNCP is then estimated by $\hat{J}(t;c)$ and the standard error of this estimator is given by

$$S(t;c) = \sqrt{\frac{\sum[v(\boldsymbol{x}) - \hat{J}]}{N(N-1)}}.$$

The standard error due to the Monte Carlo simulation can be reduced by increasing the size N of Monte Carlo samples.

When the boundary $c(s)$ is nonlinear, its BNCP can be approximated by the BNCP of a sequence of piecewise linear boundaries. In the following we give some numerical examples. First of all we are to select a piecewise linear boundary $c_n(s)$ to estimate the nonlinear boundary $c(s)$.

Example 3.1.1 (BNCP for Daniels' boundary)**.** First we consider the Daniels' boundary, which is defined as

$$c(s) = \frac{1}{2} - s\log\left(\frac{1}{4} + \frac{1}{4}\sqrt{1 + 8\exp(-\frac{1}{s})}\right), s \geq 0.$$

Since the "exact" BNCP and FPD for this boundary are known, it is used in many papers to test the computational algorithms. With $t = 1$, our result is 0.520206 ± 0.001086 with 64 partitions and simulation sample size $N = 200000$, while the exact BNCP $P_W(t;c) = 0.520251$. We run the computation on a 64-bit Windows 7 system workstation with a 3.60GHz CPU (Intel Core i7-3820) and 16GB DDR3 RAM and the computing time is 0.993175 seconds.

Example 3.1.2. Now we calculate the BNCP for some nonlinear boundaries, which have been calculated before by Loader and Deely [22] and Wang and Poetzelberger [31]. The numerical results are shown in Table 3.1 with sample size $N = 200000$ in each simulation.

Table 3.1: BNCP for some nonlinear boundaries. Standard errors are in parentheses.

$c(s)$	$n=4$	$n=8$	$n=16$	$n=32$	$n=64$
$\sqrt{1+s}$	0.804894	0.804740	0.802533	0.804751	0.804485
	(0.000799)	(0.000826)	(0.000849)	(0.000858)	(0.000867)
$0.5\sqrt{1+s}$	0.450516	0.450433	0.452872	0.449928	0.450653
	(0.000971)	(0.001019)	(0.001050)	(0.001068)	(0.001081)
$\exp(-s)$	0.439668	0.437573	0.436956	0.438864	0.439186
	(0.001047)	(0.001019)	(0.001065)	(0.001079)	(0.001088)
s^2+1	0.856445	0.852497	0.851839	0.853728	0.852372
	(0.000689)	(0.000728)	(0.000748)	(0.000759)	(0.000771)
$1+s-s^2$	0.964160	0.963216	0.963632	0.962944	0.962920
	(0.000345)	(0.000387)	(0.000372)	(0.000399)	(0.000405)

From these results we see that when the size of partitions n increases, the precision of the approximation becomes significantly better (while the computation time also increases significantly). We also find that the standard errors do not change significantly across n.

3.2 First Passage Time Density

Next we show how to calculate the FPD for piecewise linear boundaries. Similar to BNCP, equation (2.8) in Theorem 2.3.3 can be expressed as

$$g_W(t;c) = \mathrm{E}[q(W_{t_1}, W_{t_2}, \cdots, W_{t_{m-1}})], \tag{3.3}$$

where $q(\cdot)$ is given by,

$$q(x_1.x_2, \cdots, x_{m-1}) = v(x_1.x_2, \cdots, x_{m-1}) \frac{c^+_{m-1} - x_{m-1}}{\sqrt{2\pi}(t - t_{m-1})^{\frac{3}{2}}} \exp[-\frac{(c(t) - x_{m-1})^2}{2(t - t_{m-1})}]. \tag{3.4}$$

The algorithm of calculating the FPD is also similar to that for BNCP.

(1) Generate an i.i.d sample $\boldsymbol{u} = (u_1, u_2, \cdots, u_{m-1})$ from the standard Normal distribution $N(0,1)$.

(2) Compute $\boldsymbol{x} = (x_1, x_2, \cdots, x_{m-1})$ by $\boldsymbol{x} = MD^{1/2}\boldsymbol{u}$, where

$$D^{1/2} = \mathrm{diag}(\sqrt{t_1 - t_0}, \sqrt{t_2 - t_1}, \cdots, \sqrt{t_{m-1} - t_{m-2}}).$$

(3) Calculate $(c_1^+, c_2^+, \cdots, c_{m-1}^+)$, $(c_1^-, c_2^-, \cdots, c_{m-1}^-)$ and $(\beta_1, \beta_2, \cdots, \beta_{m-1})$ for the boundary.

(4) Calculate $q(\boldsymbol{x})$ by equation (3.4).

(5) Repeat steps (1)-(4) N times and calculate $\hat{J}(t;c) = \sum q(\boldsymbol{x})/N$. The density is then estimated by $\hat{J}(t;c)$ and the standard error of this estimator is given by

$$S(t;c) = \sqrt{\frac{\sum[q(\boldsymbol{x}) - \hat{J}]}{N(N-1)}}.$$

As for BNCP, we use the FPD formula for polygonal boundaries to estimate the FPD for general nonlinear boundaries.

Example 3.2.1 (FPD for square-root boundaries)**.** Square-root boundaries have been used by many authors in the literature because the "exact" FPD for these boundaries are known. We also calculate the FPD for such boundaries and the results are shown in Table 3.2 and 3.3 with sample size $N = 200000$ in each simulation. The "exact" values of FPD are from Daniels' paper [5]. These results show that our method for FDP provides good estimates. The calculated FPD with $n = 64$ and exact values in Table 3.2 are plotted in Figure 3.1. They are not distinguishable because the values are very close.

Table 3.2: The FPD for boundary $c(s) = \sqrt{1+s}$, where the values under Exact are from Daniels' paper.

t	Exact	$n = 16$	$n = 32$	$n = 64$	$n = 128$
0.2	0.2234	0.2227	0.2223	0.2230	0.2229
0.3	0.2810	0.2803	0.2799	0.2794	0.2806
0.4	0.2772	0.2772	0.2771	0.2762	0.2782
0.5	0.2559	0.2558	0.2555	0.2552	0.2561
0.6	0.2311	0.2308	0.2315	0.2318	0.2316
0.7	0.2081	0.2076	0.2070	0.2082	0.2076
0.8	0.1871	0.1867	0.1869	0.1864	0.1868
0.9	0.1685	0.1686	0.1683	0.1688	0.1690
1.0	0.1529	0.1532	0.1532	0.1524	0.1539
1.2	0.1278	0.1276	0.1277	0.1280	0.1279
1.4	0.1089	0.1089	0.1091	0.1091	0.1091
1.6	0.0946	0.0941	0.0947	0.0942	0.0944
1.8	0.0827	0.0824	0.0827	0.0827	0.0822
2.0	0.0732	0.0732	0.0732	0.0731	0.0732
2.5	0.0564	0.0564	0.0565	0.0565	0.0562
3.0	0.0455	0.0453	0.0454	0.0455	0.0452
3.5	0.0376	0.0377	0.0377	0.0375	0.0379
4.0	0.0320	0.0320	0.0320	0.0321	0.0319
4.5	0.0277	0.0277	0.0278	0.0277	0.0278
5.0	0.0243	0.0243	0.0243	0.0244	0.0244
5.5	0.0216	0.0216	0.0217	0.0216	0.0216
6.0	0.0195	0.0194	0.0194	0.0195	0.0194

Figure 3.1: The calculated FPD for boundary $c(s) = \sqrt{1+s}$, with $n = 64$.

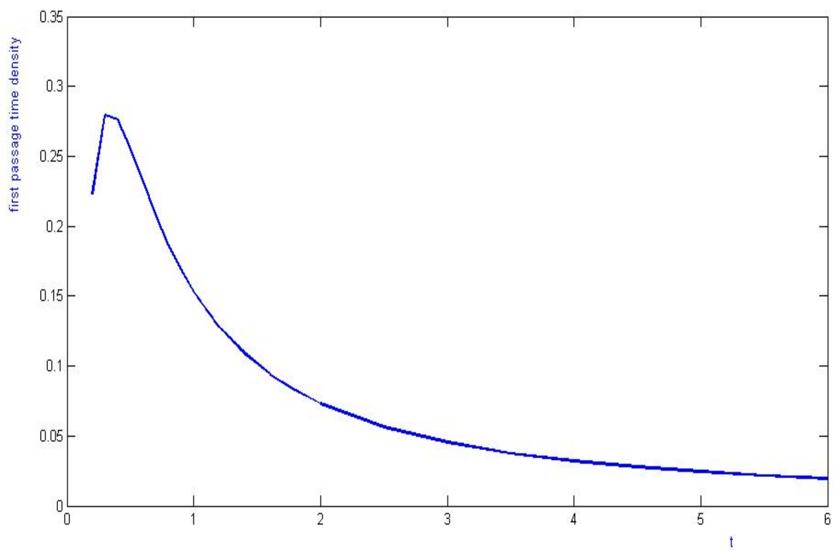

Table 3.3: The FPD for boundary $c(s) = 0.5\sqrt{1+s}$, where the values under Exact are from Daniels' paper.

t	Exact	$n = 16$	$n = 32$	$n = 64$	$n = 128$
0.05	1.2871	1.2926	1.2926	1.2890	1.2854
0.1	1.5976	1.5954	1.5954	1.5971	1.5972
0.15	1.3181	1.3173	1.3185	1.3201	1.3187
0.2	1.0570	1.0561	1.0548	1.0603	1.0568
0.25	0.8592	0.8576	0.8585	0.8556	0.8588
0.3	0.7085	0.7107	0.7087	0.7104	0.7100
0.35	0.5978	0.5996	0.5987	0.5997	0.5988
0.4	0.5137	0.5151	0.5141	0.5133	0.5140
0.45	0.4461	0.4452	0.4458	0.4465	0.4463
0.5	0.3924	0.3929	0.3929	0.3918	0.3921
0.6	0.3122	0.3120	0.3116	0.3123	0.3118
0.7	0.2568	0.2563	0.2559	0.2563	0.2563
0.8	0.2152	0.2151	0.2153	0.2140	0.2153
0.9	0.1837	0.1842	0.1843	0.1837	0.1838
1.0	0.1598	0.1597	0.1599	0.1593	0.1599
1.2	0.1253	0.1252	0.1252	0.1247	0.1252
1.4	0.1012	0.1017	0.1015	0.1023	0.1019
1.6	0.0848	0.0846	0.0844	0.0846	0.0847
1.8	0.0720	0.0719	0.0719	0.0721	0.0721
2.0	0.0621	0.0621	0.0623	0.0621	0.0622
2.2	0.0545	0.0546	0.0547	0.0542	0.0544
2.4	0.0485	0.0483	0.0484	0.0483	0.0484

When the partitions of the intervals become finer, the computation time increases significantly. From the above results we see that when t is greater than a sufficiently large value, the FPD at t is close to 0 and not significantly affected by the size of partitions n. For t at which the FPD is not close to 0, the precision of the approximation becomes significantly better as n increases.

Figure 3.2: The FPD for boundary $c(s) = 0.5\sqrt{1+s}$, with $n = 64$.

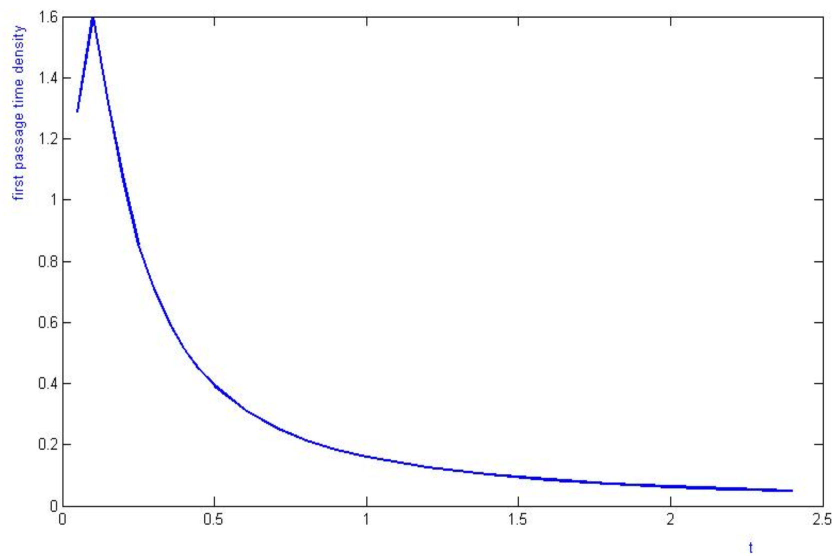

The calculated FPD and exact values with $n = 64$ in Table 3.3 are plotted in Figure 3.2. They are not distinguishable because the values are very close.

Example 3.2.2 (FPD for nonlinear boundaries)**.** Now we calculate the FPD for some nonlinear boundaries $c(s) = 1 + s^2$, $c(s) = 1 + s - s^2$ and $c(s) = \exp(-s)$. The results are shown in Table 3.4, Table 3.5 and Table 3.6 respectively. The Monte Carlo simulation sample size $N = 200000$.

Figure 3.3: The FPD for boundary $c(s) = 1 + s^2$, with $n = 64$.

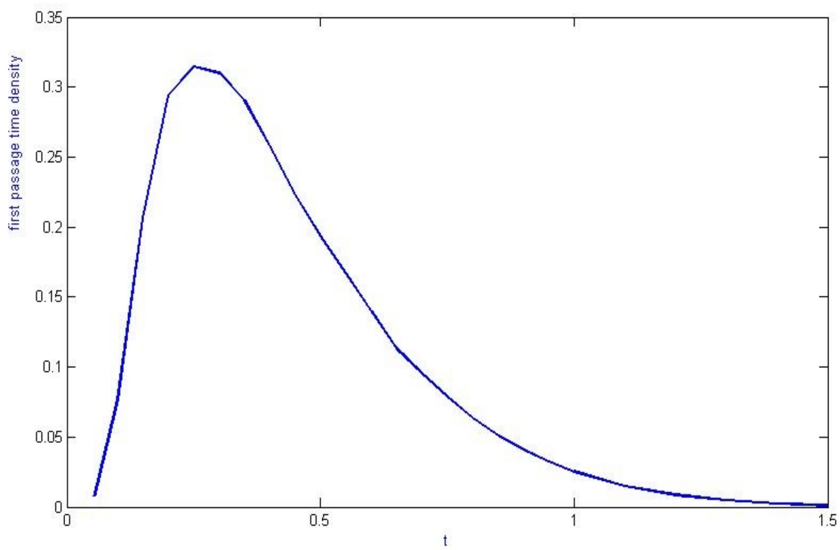

Table 3.4: The FPD for boundary $c(s) = 1 + s^2$, with $n = 64$.

t	0.05	0.10	0.15	0.20	0.25	0.30	0.35	0.40
FPD	0.0008	0.0763	0.2067	0.2941	0.3148	0.3102	0.2902	0.2583
	0.45	0.5	0.55	0.60	0.65	0.70	0.75	0.80
	0.2231	0.1932	0.1663	0.1400	0.1133	0.0956	0.0788	0.0633
	0.85	0.9	0.95	1.0	1.1	1.2	1.3	1.4
	0.0507	0.0409	0.0328	0.0255	0.0254	0.0149	0.0086	0.0049

Figure 3.4: The FPD for boundary $c(s) = 1 + s - s^2$, with $n = 64$.

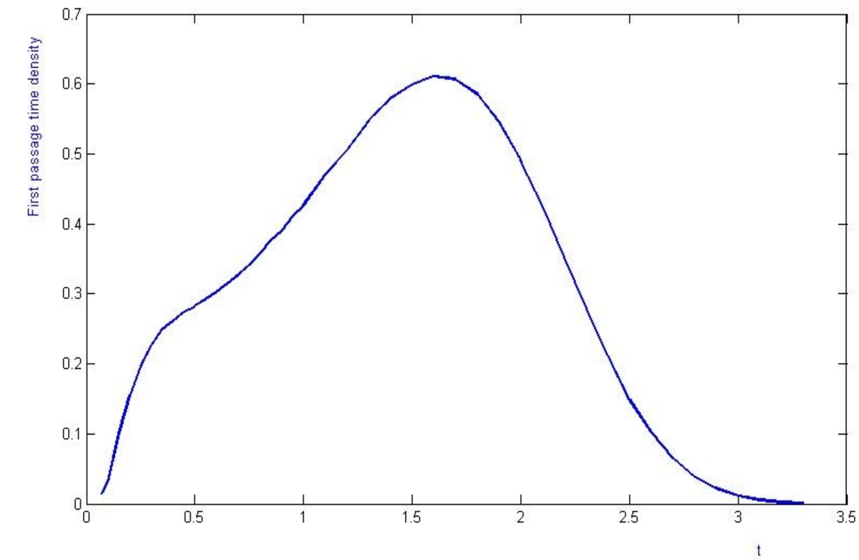

Table 3.5: The FPD for boundary $c(s) = 1 + s - s^2$, with $n = 64$.

t	0.05	0.10	0.15	0.20	0.25	0.30	0.35	0.40
FPD	0.0002	0.0317	0.1012	0.1547	0.1968	0.2267	0.2492	0.2613
	0.45	0.5	0.55	0.60	0.65	0.70	0.75	0.80
	0.2742	0.2821	0.2928	0.3024	0.3151	0.3271	0.3409	0.3580
	0.85	0.9	0.95	1.0	1.1	1.2	1.3	1.4
	0.3761	0.3894	0.4097	0.4269	0.4699	0.5046	0.5472	0.5795
	1.5	1.6	1.7	1.8	1.9	2.0	2.1	2.2
	0.5989	0.6110	0.6062	0.5850	0.5456	0.4891	0.4244	0.3526
	2.3	2.4	2.5	2.6	2.7	2.8	2.9	3.0
	0.2784	0.2115	0.1489	0.1020	0.0649	0.0386	0.0223	0.0111
	3.1	3.2	3.3	3.4	3.5			
	0.0056	0.0024	0.0010	0.0004	0.0002			

Figure 3.5: The FPD for boundary $c(s) = \exp(-s)$, with $n = 64$.

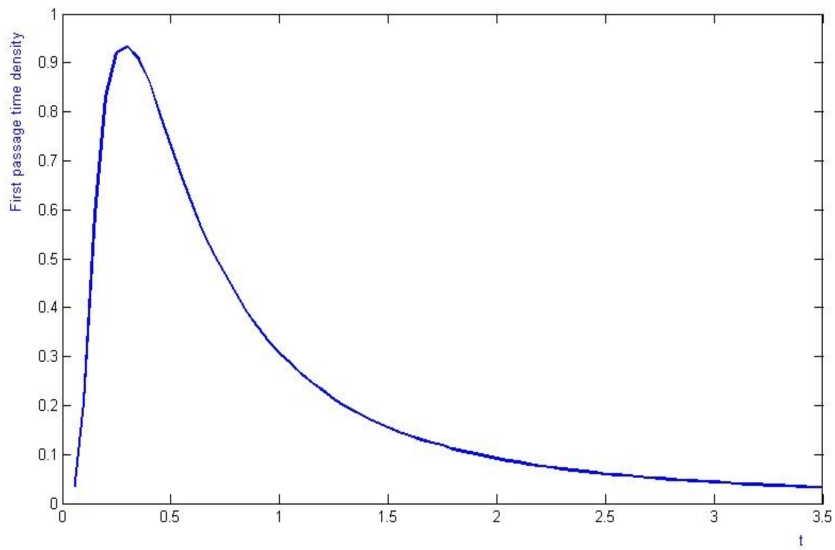

Table 3.6: The FPD for boundary $c(s) = \exp(-s)$, with $n = 64$.

t	0.05	0.10	0.15	0.20	0.25	0.30	0.35	0.40
FPD	0.0045	0.2074	0.5931	0.8312	0.9206	0.9334	0.9084	0.8632
	0.45	0.5	0.55	0.60	0.65	0.70	0.75	0.80
	0.7917	0.7289	0.6668	0.6098	0.5529	0.5055	0.4673	0.4283
	0.85	0.9	0.95	1.0	1.1	1.2	1.3	1.4
	0.3904	0.3597	0.3298	0.3063	0.2637	0.2304	0.1994	0.1743
	1.5	1.6	1.7	1.8	1.9	2.0	2.1	2.2
	0.0596	0.0571	0.0525	0.0483	0.0462	0.0434	0.0870	0.0759
	2.3	2.4	2.5	2.6	2.7	2.8	2.9	3.0
	0.0702	0.0655	0.0596	0.0571	0.0525	0.0483	0.0462	0.0434
	3.1	3.2	3.3	3.4	3.5			
	0.0406	0.0385	0.0361	0.0344	0.0324			

Finally, we note that the estimation error for both BNCP and FPD has two parts. One part is due to the approximation of the nonlinear boundary through piecewise linear boundaries. Another part is due to the approximation of Monte Carlo simulation. To reduce the standard error of Monte Carlo simulation we can increase the size of the Monte Carlo samples. The other approximation error can be reduced by increasing the size of partitions. However, more partitions will need more computation time. Since our method does not rely on equal-spaced partition, the computational cost can be reduced by considering the curvature of the boundary.

Chapter 4

Other Diffusion Processes

Many diffusion processes can be expressed as functionals of a standard Brownian motion, such as geometric Brownian motion with time dependent drift, Ornstein-Uhlenbeck processes and growth processes. In this chapter we obtain the boundary crossing probabilities and first passage time densities for such processes by applying the transformation method.

Since the transformation method for probability distribution and density is well-known, we simply present the results without detailed derivation. Instead, we refer to Wang and Poetzelberger [32].

For the simplicity of notation, in the following we denote the probability of a process $X = \{X_t, t \geq 0\}$ not crossing boundaries $a(t)$, $b(t)$ on time interval $[0, T]$ by

$$P_X(T; a, b) = P(a(t) < X_t < b(t), 0 < t \leq T),$$

and the first passage time density $g_X(T; a, b)$. When $a(t) = -\infty$, $P_X(T; a, b)$ and $g_X(T; a, b)$ will be simplified to $P_X(T; b)$ and $g_X(T; b)$ respectively.

4.1 Brownian Motion with Time Dependent Drift

Suppose $W = \{W_t, t \geq 0\}$ is a standard Brownian motion, then the Brownian motion with time dependent drift is defined as

$$X_t = \sigma W_t + \mu(t)t. \tag{4.1}$$

Corollary 4.1.1. *Let X be given by equation (4.1). Then for boundaries $a(t)$ and $b(t)$ with $a(0) < X_0 < b(0)$, we have the following two conclusions.*

(1) The BNCP for X and boundaries $a(t)$ and $b(t)$ is given by

$$P_X(T; a, b) = P_W(T; \frac{a(t) - \mu(t)t}{\sigma}, \frac{b(t) - \mu(t)t}{\sigma}).$$

(2) The FPD is given by

$$g_X(T; a, b) = g_W(T; \frac{a(t) - \mu(t)t}{\sigma}, \frac{b(t) - \mu(t)t}{\sigma}).$$

4.2 Geometric Brownian Motion

As a generalization of the classical Black-Scholes model [2] to the time-dependent interest rate process, a popular stochastic model in mathematical finance is defined by

$$\mathrm{d}X_t = r(t)X_t\mathrm{d}t + \sigma X_t\mathrm{d}W_t, \quad X_0 = x_0, \tag{4.2}$$

where $r(t) : [0, +\infty) \mapsto \mathbb{R}_+$. Then under a risk-neutral probability measure, X is a geometric Brownian motion and

$$X_t = X_0 \exp\left[R(t) - \frac{\sigma^2 t}{2} + \sigma\tilde{W}_t\right], \tag{4.3}$$

where $R(t) = \int_0^t r(u)\mathrm{d}u$ and $\tilde{W}$ is a standard Brownian motion under the same risk-neutral probability measure.

Corollary 4.2.1. *Let $X = \{X_t, t \geq 0\}$ be a geometric Brownian motion given by equation (4.3). For boundaries $a(t)$ and $b(t)$ with $a(0) < X_0 < b(0)$, define $c(t)$ and $d(t)$ as*

$$c(t) = \frac{1}{\sigma}\Big[\log\left(\frac{a(t)}{x_0}\right) + \frac{\sigma^2 t}{2} - R(t)\Big], 0 \leq t \leq T,$$

$$d(t) = \frac{1}{\sigma}\Big[\log\left(\frac{b(t)}{x_0}\right) + \frac{\sigma^2 t}{2} - R(t)\Big], 0 \leq t \leq T.$$

Then we have the following two conclusions.

(1) The BNCP for X and $a(t)$ and $b(t)$ is given by $P_X(T; a, b) = P_{\tilde{W}}(T; c, d)$.

(2) The FPD for X is given by $g_X(T; a, b) = g_{\tilde{W}}(T; c, d)$.

4.3 Ornstein-Uhlenbeck Process

Ornstein-Uhlenbeck (O-U) process is known as Vasicek model for the short -term interest rate process in mathematical finance. It is defined in state space $\mathbb{R}$ and satisfies the stochastic differential equation

$$\mathrm{d}X_t = \kappa(\alpha - X_t)\mathrm{d}t + \sigma \mathrm{d}W_t, \qquad X_0 = x_0, \tag{4.4}$$

where $\kappa, \sigma \in \mathbb{R}_+$ and $\alpha \in \mathbb{R}_+$ are constants.

Corollary 4.3.1. *Let $X = \{X_t, t \geq 0\}$ be an O-U process given by equation (4.4). Then for boundaries $a(t)$ and $b(t)$ with $a(0) < X_0 < b(0)$, define $c(s)$ and $d(s)$ as*

$$c(s) = \alpha - x_0 + [a(t(s)) - \alpha]\left(1 + \frac{2\kappa s}{\sigma^2}\right)^{1/2},$$

$$d(s) = \alpha - x_0 + [b(t(s)) - \alpha]\left(1 + \frac{2\kappa s}{\sigma^2}\right)^{1/2},$$

where

$$t(s) = \frac{1}{2\kappa} log\left(1 + \frac{2\kappa s}{\sigma^2}\right), s \geq 0.$$

Then we have the following two conclusions.

(1) The BNCP for X and $a(t)$ and $b(t)$ is given by $P_X(T; a, b) = P_W(S; c, d)$, where $S = \sigma^2(\exp(2\kappa T) - 1)/2\kappa$.

(2) The FPD for X is given by $g_X(T; a, b) = \sigma^2 \exp(2\kappa T) g_W(S; c, d)$.

Example 4.3.2. Now we consider an example of O-U process X crossing constant boundaries $a(t) = -\infty$ and $b(t) = h > 0$. In this case $c(s) = -\infty$ and

$$d(s) = \alpha - x_0 + (h - \alpha)\left(1 + \frac{2\kappa s}{\sigma^2}\right)^{\frac{1}{2}}.$$

In particular, set $\alpha = x_0$, $\sigma^2 = 2\kappa = 1$ and $h = x_0 + 1$. Then we have $d(s) = \sqrt{1+s}$ for $0 \leq s \leq S = e^T - 1$. Therefore $P_X(T; h) = P_W(S; \sqrt{1+s})$ and $g_X(T; h) = \exp(T) g_W(S; \sqrt{1+s})$. Note that the case of BM crossing square-root boundary $\sqrt{1+s}$ has been calculated in Chapter 3.

4.4 Growth Process

Growth process is an important stochastic model in population genetics [26]. It satisfies

$$\mathrm{d}X_t = (\alpha X_t - \beta X_t \log X_t)\mathrm{d}t + \sigma X_t \mathrm{d}W_t, \qquad X_0 = x_0 \tag{4.5}$$

on state space $\mathbb{R}_+$, where α, β and σ are positive constants.

Corollary 4.4.1. *Let $X = \{X_t, t \geq 0\}$ be a growth process. For boundaries $a(t)$ and $b(t)$ with $a(0) < X_0 < b(0)$, define $c(s)$ and $d(s)$ as*

$$c(s) = \frac{\sqrt{1+2\beta s}}{\sigma}\big[\log a(t(s)) + \frac{\sigma^2 - 2\alpha}{2\beta}\big] - \frac{1}{\sigma}\big[\log x_0 + \frac{\sigma^2 - 2\alpha}{2\beta}\big],$$

$$d(s) = \frac{\sqrt{1+2\beta s}}{\sigma}\big[\log b(t(s)) + \frac{\sigma^2 - 2\alpha}{2\beta}\big] - \frac{1}{\sigma}\big[\log x_0 + \frac{\sigma^2 - 2\alpha}{2\beta}\big],$$

Then we have the following two conclusions.

(1) The BNCP for X and $a(t)$ and $b(t)$ is given by $P_X(T; a, b) = P_W(S; c, d)$, where $S = (\exp(2\beta T) - 1)/2\beta$.

(2) The FPD for X is given by $g_X(T; a, b) = \exp(2\beta T) g_W(S; c, d)$.

Example 4.4.2. Now we consider an example of growth process X crossing constant boundaries $a(t) = 0$ and $b(t) = h > 0$. In this case $c(s) = -\infty$ and

$$d(s) = \frac{1+2\beta s}{\sigma}\big(\log h + \frac{\sigma^2 - 2\alpha}{2\beta}\big) - \frac{1}{\sigma}\big(\log x_0 + \frac{\sigma^2 - 2\alpha}{2\beta}\big).$$

In particular if we take $\sigma^2 = 2\alpha$, $\beta = 0.5$, $x_0 = 1$ and $h = e^\sigma$, we will obtain $d(s) = \sqrt{1+s}$ and $S = e^T - 1$. Then $P_X(T; 0, h) = P_W(S; \sqrt{1+s})$ and $g_X(T; 0, h) = \exp(T) g_W(S; \sqrt{1+s})$.

Chapter 5

Summary

In this thesis we have studied boundary crossing probabilities and first passage time densities for Brownian motion and various types of boundaries.

The main objects are to find explicit formula for the first passage time distributions and to develop algorithms to numerically calculate the distributions. We first extended the known boundary crossing probabilities formula for continuous piecewise linear boundaries to discontinuous piecewise linear boundaries. This explicit formula can be used to approximate the boundary crossing probabilities for general nonlinear boundaries. Using this approach, the approximation error can be assessed or even controlled before the real computation starts. As a by product, we have also derived the formula for the boundary crossing probabilities for the Brownian bridge.

Furthermore, an explicit formula for the first passage time densities is derived for piecewise linear boundaries. The approach to compute the first passage time densities is similar with the approach for the boundary crossing probabilities.

Although the results in this thesis are given for one-sided boundaries, most of them can be extended to two-sided boundaries. This approach can be applied to a class of diffusion processes which can be expressed as piecewise monotone functionals of Brownian motion, including geometric Brownian motion, O-U processes and growth processes.

Appendix

We include the MatLab functions that are used to calculate numerical examples in this thesis.

A1: Function for the BCP for BM and linear piecewise boundaries

```
function [EBCPDC SDBCPDC]=BcpLP3(BoundValS,RunTimes)
% file name BcpLP3
% This function is to canculate the BCP of stardard BM
 % Boudary is LINEAR PIECEWISE Boundary
% Version 2012-11-16
% Define Parameters
 % BoundVal =[Break Points; Boundary Right Limit at Points; ...
 %                                Boundary Left Limit at Points].
   % Break Points : beginning with 0 and ending with EndPoint.
   % BoundVal has to be 3*(n+1) matrix.
 %   RunTimes: Repeat times.
[sizen,sizem]=size(BoundValS);
sizem=sizem-1;
```

```
if sizem==1
  T=BoundValS(1,2);
  a=(BoundValS(3,2)-BoundValS(3,1))/BoundValS(1,2);
  b=BoundValS(3,1);
  EBCPDC=normcdf((a*T+b)/sqrt(T))-exp(-2*a*b)*normcdf((a*T-b)/sqrt(T));
  SDBCPDC=0;
else
  dt=diff(BoundValS(1,:));% dt is each length of pieces of Boundary.
  DTI=diag(1./dt);
  SDT=diag(sqrt(dt));
  giterm=RunTimes;
  nullgm=((1:giterm)*0)';
  % VALBegin is the right-limit of each boundary piece at points.
  VALSBegin=(nullgm+1)*BoundValS(2,:);
  % VALEnd is the Left-limit of each boundary piece at the end points.
  VALSEnd=(nullgm+1)*BoundValS(3,:);
  ii=1:giterm;
  gi=nullgm;
        x=randn(giterm,sizem)*SDT;
        sumx=cumsum(x')';
        BBegin=VALSBegin-[nullgm sumx];
        BEnd=VALSEnd-[nullgm sumx];
        Bmin=min(BBegin,BEnd);
        Bm=min(Bmin')';
        ip=ii(Bm>0);
```

```
            Q=-2*BBegin(ip,1:sizem).*BEnd(ip,2:(sizem+1))*DTI;
            ExpQ=exp(Q);
            gv=1-ExpQ;
            gp=prod(gv')';
            gi(ip,1)=gp;
  EBCPDC=mean(gi);
  SDBCPDC=sqrt(var(gi)/RunTimes);
end
```

A2: Function for the BCP for BM and nonlinear boundaries

```
function [EBCP SDBCP]=BcpC(mybou,EndPoint,DivParts,RunTimes)
% File name BcpC
% This function is to canculate the BCP of stardard BM
  % Boudary is General Continuous Boundary
% Version 2012-11-16
% Define Parameters
  % EndPoint: Process on [0,EndPoint]
  % DivParts: How many partations we divide the boundary.
  % RunTimes: Repeat times.
% In this funtion: mybou is a self-difined function to get the boundary.
  % Use function handle.
  % Example: boundary f(t)=exp(-t)
tau=EndPoint;
ts=linspace(0,tau,DivParts+1);
lengthm=length(ts);
```

```
Val=mybou(ts);
  % Example: Val=exp(-ts);
[EBCP SDBCP]=BcpLP3([ts;Val;Val],RunTimes);
```

A3: Function for the BCP for BM and nonlinear boundaries

This m file is to canculate the BCP for BM and boundary $c(t) = exp(-t)$ for example. With $T = 1$ we divide $[0, T]$ into 32 parts. The Monte carlo simulation sample size is 200000.

```
% Parameters values used
EndPoint=1;
DivParts=32;
RunTimes=200000;
% Change the Parameters values to apply for other cases.
tau=EndPoint;
ts=linspace(0,tau,DivParts+1);
lengthm=length(ts);
  Val=exp(-ts);
[EBCP SDBCP]=BcpLP3([ts;Val;Val],RunTimes);
```

A4: Function for the BCP for O-U process and linear piecewise boundaries

```
function [EBCPOU SDBCPOU]=OuBcpLP(BoundValS,OUP,RunTimes)
% Filename: OuBcpLP
```

```
% This function is to canculate the BCP of a Ornstein-Uhlenbeck Process
  % Boudary is LINEAR PIECEWISE Boundary
% Version 2012-11-16
% Define Parameters
  % OUP: the parameter vector of the OU process
     % The parameters of the OU process is kappa, alpha, sigma, x0
     % OUP=[kappa,alpha,sigma,x0];
  % BoundValS =[Break Points; Boundary Right Limit at Points);...
  %                                 Boundary Left Limit at Points].
     % BoundValS has to be 3*(n+1) matrix.
  % RunTimes: Repeat times.
[sizen,sizem]=size(BoundValS);
kappa=OUP(1);
alpha=OUP(2);
sigma=OUP(3);
x0=OUP(4);
NewBoundVal=ones(sizen,sizem);
NewBoundVal(1,:)=0.5*sigma^2*(exp(2*kappa*BoundValS(1,:))-1)/kappa;
NewBoundVal(2,:)=alpha-x0+exp(kappa*BoundValS(1,:)).*(BoundValS(2,:)-alpha);
NewBoundVal(3,:)=alpha-x0+exp(kappa*BoundValS(1,:)).*(BoundValS(3,:)-alpha);
[EBCPOU SDBCPOU]=BcpLP3(NewBoundVal,RunTimes);
```

A5: Function for the BCP for O-U process and nonlinear boundaries

```
function [EBCP SDBCP]=OuBcpC(mybou,EndPoint,DivParts,OUP,RunTimes)
% Filename: OuBcpC
% This function is to canculate the BCP of Ornstein-Uhlenbeck Process
  % Boudary is General Continuous Boundary
% Version 2012-11-20
% Define Parameters
  %   OUP: the parameter vector of the OU process
    % The parameters of the OU process is kappa, alpha, sigma, x0
    % OUP=[kappa,alpha,sigma,x0];
 % EndPoint: Process on [0,EndPoint]
 % DivParts: How many partations we divide the boundary.
 % RunTimes: Repeat times.
% In this funtion: mybou is a self-difined function to get the boundary.
  % Example: boundary f(t)=exp(-t)
tau=EndPoint;
ts=linspace(0,tau,DivParts+1);
lengthm=length(ts);
Val=mybou(ts);
  % Example: Val=exp(-ts);
[EBCP SDBCP]=OuBcpLP([ts;Val;Val],OUP,RunTimes);
```

A6: Function for the BCP for geometric Brownian motion and linear piecewise boundaries

```
function [EBCPOU SDBCPOU]=GBcpLP(BoundValS,GP,RunTimes)
% File name: GBcpLP
% This function is to canculate the BCP of a Geoetric Brownian Motion
 % Boudary is LINEAR PIECEWISE Boundary
% Version 2012-11-20
% Define Parameters
 %   GP: the parameter vector of the Geoetric Brownian Motion
    % The parameters of the GP process is mu, sigma, y0
    % GP=[mu, sigma, y0];
 % BoundValS =[Break Points; Boundary Right Limit at Points); ...
 %                  Boundary Left Limit at Points].
    % BoundValS has to be 3*(n+1) matrix.
 % RunTimes: Repeat times.
[sizen,sizem]=size(BoundValS);
mu=GP(1);
sigma=GP(2);
y0=GP(3);
NewBoundVal=ones(sizen,sizem);
NewBoundVal(1,:)=BoundValS(1,:);
NewBoundVal(2,:)=(log(BoundValS(2,:))-log(y0)-(u-0.5*sigma^2))/sigma;
NewBoundVal(3,:)=(log(BoundValS(3,:))-log(y0)-(u-0.5*sigma^2))/sigma;
[EBCPOU SDBCPOU]=BcpLP3(NewBoundVal,RunTimes);
```

A7: Function for the BCP for geometric Brownian motion and nonlinear boundaries

```
function [EBCPOU SDBCPOU]=GBcpC(mybou,EndPoint,DivParts,GP,RunTimes)
% File name: GBcpC
% This function is to canculate the BCP of a Geoetric Brownian Motion
 % Boudary is General Continuous Boundary
% Version 2012-11-20
% Define Parameters
 %   GP: the parameter vector of the OU process
    % The parameters of the OU process is kappa, alpha, sigma, x0
    % GP=[kappa,alpha,sigma,x0];
 % EndPoint: Process on [0,EndPoint]
 % DivParts: How many partations we divide the boundary.
 % RunTimes: Repeat times.
% In this funtion: mybou is a self-difined function to get the boundary.
  % Example: boundary f(t)=exp(-t)
tau=EndPoint;
ts=linspace(0,tau,DivParts+1);
lengthm=lenth(ts)
Val=mybou(ts);
  % Example: Val=exp(-ts);
[EBCP SDBCP]=GBcpLP([ts;Val;Val],GP,RunTimes);
```

A8: Function for the FPD for BM and linear piecewise boundaries

```
function EBCDL=fcdLPf(BoundVals,RunTimes)
% File name: fcdLPf
% This function is to canculate the First Crossing-time Density of stardard BM
 % Boudary is LINEAR PIECEWISE Boundary
% Version 2014-01-16
   % This is the final version
% Define Parameters
   % BoundVal =[Break Points; Boundary Values].
       % BoundVal has to be 2*(n+1) matrix.
   % RunTimes: Repeat times.
% ss is a parameter defined inside.
ss=2000;
[sizen,sizem]=size(BoundVals);
sizem=sizem-1;
giterm=RunTimes;
nullgm=((1:giterm)*0)';
dt=diff(BoundVals(1,:));
    % dt is each length of pieces of Boundary.
DT=diag(dt);
DTI=diag(1./dt(1:sizem-1));
SDT=diag(sqrt(dt(1:sizem-1)));
dB=diff(BoundVals(2,:));
Beta=(nullgm+1)*BoundVals(2,1:sizem);
```

```
Rg=[];
for i=1:1:ss
    x=randn(giterm,sizem-1)*SDT;
    sumx=cumsum(x')';
    ii=1:giterm;
    gi=nullgm;
      B=Beta-[nullgm sumx];
      Bm=min(B')';
      ip=ii(Bm>0);
       Q=-2*B(ip,1:sizem-1).*B(ip,2:sizem)*DTI;
       ExpQ=exp(Q);
       gv=1-ExpQ(:,1:sizem-1);
       gp1=prod(gv')';
       gp2=1/sqrt(2*pi*dt(sizem)^3)*(BoundVals(2,sizem)-sumx(ip, ...
       sizem-1)).*exp(-0.5*(BoundVals(2,sizem+1)-sumx(ip,sizem-1)).^2/dt(sizem));
       gp=gp1.*gp2;
     gi(ip,1)=gp;
     Mgi=mean(gi);
     Rg=[Rg Mgi];
end
EBCDL=mean(Rg);
```

A8: Function for the BCP for BM with jumps and linear piecewise boundaries where the jump process follows a Poisson process

Note that the boundary is defined in function mybou and the jump hights in defined in function myjphm.

```
function [EZYBCP SDBCP]=BcpLJ(LBP,lambda,EndPoint,RunTimes,myjphm)
% Filename: BcpLJ
% This function is to canculate BCP of BM with jumps.
 % Boudary is LINEAR Boundary
% Version 2012-11-16
% Define Parameters
 %   lambda: Possion Process prameter
 %   EndPoint: Process on [0,EndPoint]
 %   RunTimes: Repeat times.
 %   LBP: Linear Boundary Parameters;
     % LBP=[slope intercept];
% I write one functions (m file) to support this function
 % function myjph. To get jump hights.
      % Example: Use Double EXP distribution here.
Pprijump=[];
for iim=1:1:RunTimes
    m=poissrnd(lambda*EndPoint); % use m as the numbers of Jumps.
      % Determine the time when jumps happen.
    tau=EndPoint; % Use tau to replace EndPoint
```

```
    ts1=unifrnd(0,tau,[1,m]);
    ts1=sort(ts1);
      % Deal with boudary. Partition.
    ts2=[0 1];
    ts3=union(ts1,ts2);
      % NOTICE: There can be the same values in ts1 and ts2; so get union.
    ts=sort(ts3);
    le=length(ts);
      % Get Orignal Boundary
    oldbi=LBP(1)*ts+LBP(2); % Example: f(t)=1.5t-0.5;
    if m==0
        Pri=BcpLP3([ts;oldbi;oldbi],1);
    else
      % Get the hights of Jumps.
    jh=myjphm(m);
      % jh are the hights of every jump.
    bi1b=oldbi-sum((repmat(ts,m,1)>=repmat(ts1',1,le)).*repmat(jh',1,le));
      %bi1b: after jump:  beginning
    bi2e=oldbi-sum((repmat(ts,m,1)>repmat(ts1',1,le)).*repmat(jh',1,le));
      %bi2e: before jump: ending
    Pri=BcpLP3([ts;bi1b;bi2e],1);
    end
    Pprijump=[Pprijump Pri];
end
EZYBCP=mean(Pprijump);
```

```
SDBCP=sqrt(var(Pprijump)/RunTimes);
```

A8: Function for the BCP for BM with jumps and nonlinear boundaries where the jump process follows a Poisson process

```
function [EZYBCP SDBCP]=BcpCJ(mybou,lambda,EndPoint,RunTimes,DivParts,myjphm)
% This function is to canculate BCP of BM with jumps.
% File name:BcpCJ
 % Boudary is General Continuous Boundary
% Version 2012-11-16
% Define Parameters
  %   lambda: Possion Process prameter
  %   EndPoint: Process on [0,EndPoint]
  %   RunTimes: Repeat times.
  %   DivParts: How many partations we divide the boundary.
%  I write two functions (m file) to support this function
  % Use function handle.
  % function 1 mybou: To get Boundary.
      %    Example: f(t)=sqrt(t+1);
  % function 2 myjphm: To get jump hights.
      %    Example: Use Double EXP distribution here.
Pprijump=[];
for iim=1:1:RunTimes
  m=poissrnd(lambda*EndPoint);% use m as the numbers of Jumps.
  if m==0
```

```
  ts=linspace(0,EndPoint,DivParts+1);
  oldbi=mybou(ts);
  Pri=BcpLP3([ts;oldbi;oldbi],1);
else
    % Determine the time when jumps happen.
  tau=EndPoint; % Use tau to replace T
  ts1=unifrnd(0,tau,[1,m]);
  ts1=sort(ts1);
    % Deal with boudary. Partition.
  ts2=linspace(0,tau,DivParts+1);
  ts3=union(ts1,ts2);
    % NOTICE: There can be the same numbers in ts1 and ts2, use union here.
  ts=sort(ts3);
  le=length(ts);
    % Bouldary.
  oldbi=mybou(ts); % Example:oldbi=sqrt(ts+1);
    % Get the hights of Jumps.
  jh=myjphm(m); % jh are the hights of every jump.
    % Example: Double EXP distribution.
      % jh=randdexp(0.5,0.02,0.03,1,m)/0.2;
      % I write a function 'randdexp' to get a random double exp number
    % Get Boundary including jumps.
  bi1b=oldbi-sum((repmat(ts,m,1)>=repmat(ts1',1,le)).*repmat(jh',1,le));
    %bi1b: after jump:  beginning
  bi2e=oldbi-sum((repmat(ts,m,1)>repmat(ts1',1,le)).*repmat(jh',1,le));
```

```
      %bi2e: before jump: ending
    Pri=BcpLP3([ts;bi1b;bi2e],1);
  end
  Pprijump=[Pprijump Pri];
end
EZYBCP=mean(Pprijump);
SDBCP=sqrt(var(Pprijump)/RunTimes);
```

Bibliography

[1] P. Billingsley (1986). *Probability and Measure*, Second Edition. Wiley, New York.

[2] F. Black and M. Scholes (1973). The pricing of options and corporate liabilities. *J. Plitical Economy*, 81, 637-659 45

[3] H. Charles and J.S. Dukes (2009). Effects of warming and altered precipitation on plant and nutrient dynamics of a new england salt marsh. *Ecological Applications*, 19, 1758-1773. 1

[4] J. Durbin (1971). Boundary crossing probabilities for the Brownian motion and Poisson processes and techniques for computing the power of the kolmogorov-smirnov test . *Journal of Applied Probability* , 8 (3) , 431-453 4

[5] H. E. Daniels (1996). Approximating the First Crossing-Time Density for a Curved Boundary. *Bernoulli*, 2 (2), 133-143. 3, 10, 11, 35

[6] A. Einstein (1905). Investigations on the Theory of Brownian Movement. *Anuuleu der Physik*, 17, 549-560. 7

[7] B. Ferebee (1983). An asymptotic expansion for one-sided Brownian exit densities. *Probability Theory and Related Fields*, Volume 63, Issue 1, 1-15 3

[8] E. Garshick, F. Laden, J. E. Hart, B. Rosner, T. J. Smith, D. W. Dockery and F. E. Speizer (2004). Assessing lung cancer risk in railroad workers using a first hitting time regression model *Environmental Health Perspectives*, Vol. 112, No.15, 1539-1543. 1

[9] A. P. Ghosh (2011). *Backward and Forward Equations for Diffusion Processes*, Wiley Encyclopedia of Operations Research and Management Science. 10

[10] P. Hieber, and M. Scherer J (2010). Efficiently pricing barrier options in a Markov-switching framework. *Computational Applied Mathematics*, 235(3), 679-685. 1

[11] J. C. Horrocks and M. E. Thompson (2004). Modelling event times with multiple outcomes using the Wiener process with drift. *Lifetime Data Anal*, 10, 29-49. 1

[12] T. Ichiba, C. Kardaras (2011). Efficient estimation of one-dimensional diffusion first passage time densities via Monte Carlo simulation. *Applied Probability Trust*. 48, 699-712. 4

[13] M. Jeannin. and M. Pistorius (2010). A transform approach to compute prices and Greeks of barrier options driven by a class of Lvy processes. *Quant. Finance*, 10, 629-644. 1

[14] Y. Jiang , Z. Zhang , T. V. Voorhis , J. D. Mccalley (2003). Risk-based Maintenance Optimization for Transmission Equipment. *IEEE Transactions on Power System*, Vol.21, No.3, 1191-1200. 1

[15] D. Jun (2013). Pricing Chained Options with Curved Barriers *Mathematical Finance* 23, 4, 763-776 1

[16] I. Karatzas and S. E. Shreve (1991). Brownian motion and stochastic calculus, *Graduate Texts in Mathematics*, Vol. 113, Springer-Verlag, New York, second ed.

[17] S. Karlin and H. Taylor (1975). *A First Course in Stochastic Processes*, 2nd edn. Academic Press, New York.

[18] S. G. Kou and H. Wang (2003). First Passage Times of a Jump Diffusion Process. *Advances in Applied Probability*, Vol.35, No.2, 504-531.

[19] G. F. Lawler (2006). *Introduction to Stochastic Processes*, Second Edition. Chapman and Hall/CRC, Boca Raton, FL. 1

[20] H. R. Lerche (1986). Boundary Crossing of Brownian Motion. *Lecture Notes in Statistics* 40. 10

[21] X. S. Lin (1999). Laplace Transform and Barrier Hitting Time Distributions. *Lifetime Data Anal*, 1, 165-177. 3

[22] C. R. Loader and J. J. Deely (1987). Computations of boundary crossing probabilities for the Wiener process. *J. Statist. Comput. Simul*, 27, 95-105 3

[23] S. A.K. Metwally and A. F. Atiya (2002). Using Brownian Bridge for Fast Simulation of Jump-Diffusion Processes and Barrier Options. *Journal of Derivatives*. Vol. 10, No. 1, 43-54. 33

[24] A. Molinia, P. Talknerc, G. G. Katulb, A. Porporatoa (2011). First passage time statistics of Brownian motion with purely time dependent drift and diffusion. *Physica A: Statistical Mechanics and its Applications*, 390, 1841-1852. 4

[25] K. Moon (2008). Efficient Monte Carlo algorithm for pricing Barrier options. *Commun. Korean Math.* 23(23), 285-294.

[26] L. M. Ricciardi, A. Di Crescenzo, V. Giorno, and A.G. Nobile (1999). An outline of theoretical and algorithmic approaches to first passage time problems with applications to biological modeling. *Mathematica Japonica*, 50, 247C322. 4

[27] V. S.F. Lo, G. O. Roberts, and H. E. Daniels (2002). Inverse method of images. *Bernoulli*Volume 8, Number 1 53-80. 47

[28] D. Siegmund (1986). Boundary Crossing Probabilities and Statistical Applications. *The Annals of Statistics*. Vol. 14, No. 2 , 361-404 3

4, 12

[29] J. Stachel (2005). Einsteins Miraculous Year. *Princeton University Press*, Princeton, NJ, 7

[30] V. Strassen (1967). Almost sure behaviour of sums of independent random variables and martingales. *Math. Statist. and Prob.*, Vol. 2, Pt. 1 , 315-343 3

[31] L. Wang and K. Poetzelberger (1997). Boundary crossing probability for brownian motion and general boundaries. *Applied Probability Trust*, 34, 54-65. 6, 12, 15, 18, 29, 33

[32] L. Wang and K. Poetzelberger (2007). Crossing probability for some diffusion processes with piecewise continuous boundaries. *Methodology and Computing in Applied Probability*, 9, 21-40 44